This is the peer-reviewed, final accepted version for American Mineralogist, published by the Mineralogical Society of America.
The published version is subject to change. Cite as Authors (Year) Title. American Mineralogist, in press.
DOI: https://doi.org/10.2138/am-2022-8329. http://www.minsocam.org/

Revision #2—10 January 2022—Submitted to *American Mineralogist*

An evolutionary system of mineralogy, Part VI: Earth's earliest Hadean crust (> 4370 Ma)

SHAUNNA M. MORRISON[1], ANIRUDH PRABHU[1], AND ROBERT M. HAZEN[1,*]

[1]Earth and Planets Laboratory, Carnegie Institution for Science,
5251 Broad Branch Road NW, Washington DC 20015, U. S. A.

ABSTRACT

Part VI of the evolutionary system of mineralogy catalogs 262 kinds of minerals, formed by 18 different processes, that we suggest represent the earliest solid phases in Earth's crust. All of these minerals likely formed during the first tens of millions of years following the global-scale disruption of the Moon-forming impact prior to ~4.4 Ga, though no samples of terrestrial minerals older than ~4.37 Ga are known to have survived on Earth today. Our catalog of the earliest Hadean species includes 80 primary phases associated with ultramafic and mafic igneous rocks, as well as more than 80 minerals deposited from immiscible S-rich fluids and late-stage Si-rich residual melts. Earth's earliest crustal minerals also included more than 200 secondary phases of these primary minerals that were generated by thermal metamorphism, aqueous alteration, impacts, and other processes. In particular, secondary mineralization related to pervasive near-surface aqueous fluids may have included serpentinization of mafic and ultramafic rocks, hot springs and submarine volcanic vent mineralization, hydrothermal sulfide deposits, zeolite and associated mineral formation in basaltic cavities, marine authigenesis, and hydration of subaerial lithologies. Additional Hadean minerals may have formed by thermal metamorphism of lava xenoliths, sublimation at volcanic fumaroles, impact processes, and

volcanic lightning. These minerals would have occurred along with more than 180 additional phases found in the variety of meteorites that continuously fell to Earth's surface during the early Hadean Eon.

***E-mail:** rhazen@carnegiescience.edu.

ORCID 0000-0003-4163-8644

Keywords: philosophy of mineralogy; classification; mineral evolution; Hadean Eon; igneous rocks; aqueous alteration; magma ocean; mineral network graphs

This is the peer-reviewed, final accepted version for American Mineralogist, published by the Mineralogical Society of America.
The published version is subject to change. Cite as Authors (Year) Title. American Mineralogist, in press.
DOI: https://doi.org/10.2138/am-2022-8329. http://www.minsocam.org/

INTRODUCTION

The evolutionary system of mineralogy is an effort to place the > 5700 mineral species approved by the International Mineralogical Association's Commission on New Minerals, Nomenclature, and Classification (IMA-CNMNC; https://rruff.info/ima, accessed 17 September 2021) into their historical and paragenetic contexts (Hazen 2019; Cleland et al. 2021; Hazen and Morrison 2022; Hazen et al. 2022). Parts I through V of the system detailed almost 300 species that occur as primary and secondary phases in meteorites (Hazen and Morrison 2020, 2021a; Morrison and Hazen 2020, 2021; Hazen et al. 2021). Thanks to decades of intensive mineralogical investigations, these earliest stages of mineral evolution are well documented.

An important aspiration of the evolutionary system of mineralogy has been to enumerate "historical natural kinds," which ideally represent "genuine divisions of nature" that arose through well-defined historical processes (Boyd 1991, 1999; Hawley and Bird 2011; Magnus 2012; Khalidi 2013; Ereshevsky 2014; Godman 2019; Cleland et al. 2021). In most instances, we attempt to classify mineral natural kinds on the basis of the distinctive combinations of chemical and physical attributes of natural specimens – properties that arose as a consequence of numerous different paragenetic modes (Hazen and Morrison 2022). Thus, for example, the trace elements, isotopes, fluid and solid inclusions, morphologies, petrologic contexts, and other attributes of pyrite (FeS_2) from hydrothermal vein deposits are strikingly different from pyrite formed by authigenesis or biogenic processes (Gregory et al. 2019) – characteristics that point to more than 20 natural kinds of pyrite (Hazen and Morrison 2022). The evolutionary system is based on those diagnostic, information-rich aspects of mineral specimens, thus complementing standard protocols of the IMA-CNMNC, which define mineral "species" based on unique combinations of major element chemical composition and idealized atomic structure (e.g., Burke

2006; Mills et al. 2009; Schertl et al. 2018; Hatert et al. 2021; Hazen 2021; Hawthorne et al. 2021).

Because the evolutionary system focuses on the changing diversity and distribution of minerals through space and time, it considers any solid phases that likely occurred during the formation and evolution of Earth's near-surface environment. While many of the most ancient minerals are preserved in meteorites, others, including nebular ices and the earliest phases that composed the terrestrial crust, are not. Here we focus on those hypothetical first solid phases formed at or near Earth's surface after its initial accretion and differentiation (> ~4.56 Ga), as well as the earliest minerals to condense following the postulated catastrophic Moon-forming event at > 4.4 Ga and its dynamic aftermath. No known terrestrial minerals survive from Earth's first 190 million years; the oldest reported sample is a detrital zircon grain from 4.374 ± 0.006 Ga (Valley et al. 2014). Consequently, this part of the evolutionary system will remain the most speculative stage of our planet's mineral evolution. Barring the discovery of meteorites ejected from Earth's surface during the > 100-million-year window before the Moon-forming impact, or from the period of initial cooling in the few tens of millions of years after that event (Armstrong et al. 2002; Crawford et al. 2008; Bellucci et al. 2019), the crustal mineralogy of the earliest Hadean Eon will remain a theoretical pursuit (Hazen 2013; Morrison et al. 2018; Hazen and Morrison 2021b).

In spite of this lack of tangible evidence of Earth's earliest Hadean mineralogy, convincing constraints are provided by insights from experimental petrology, isotope geochemistry, and theoretical modeling of magma ocean behavior, coupled with observations of the primitive mineralogy of Mars, Mercury, the Moon, and other rocky objects of the solar system.

Accordingly, in this contribution we offer a hypothetical introduction to Earth's earliest mineralogy – an enigmatic subject that must have unfolded in at least two major episodes.

The initial accretion of Earth and other planets occurred > 4.56 Ga ago during the solar nebula's first several million years (Burkhardt et al. 2011; Budde et al. 2016; Kruijer et al. 2017; Desch et al. 2018), followed by a prolonged period of differentiation and crustal formation (Moynier et al. 2010; Kruijer et al. 2014; Badro and Walter 2015; Trønnes et al. 2019). In many respects, the earliest terrestrial minerals must have mirrored the ~120 primary and secondary asteroidal phases found in the mafic and ultramafic lithologies of stony achondrite meteorites, which represent fragments of crusts and mantles from the earliest differentiated planetessimals of the solar system (> 4.55 Ga; Morrison and Hazen 2021; Hazen and Morrison 2021a). It is also likely that additional mineralogical diversity emerged through varied fluid-rock reactions in the Hadean crust, as well as alteration of subaerial deposits by impacts, evaporation, lightning, and photo-reactions, as the earliest Earth developed a dense atmosphere and dynamic hydrosphere (Abe 1993; Wilde et al. 2001; Mojzsis et al. 2001; Schaefer and Fegley 2010; Zahnle et al. 2010; Elkins-Tanton 2011: Hazen and Morrison 2022).

A second major episode of *de nova* mineralization followed cooling of the globe-spanning magma ocean that was a consequence of the Moon-forming impact at > 4.4 Ga. That dramatic time of mineral obliteration was prelude to an extended period of crustal solidification and earliest effects of aqueous and thermal alteration – mineral-forming processes that are the focus of this contribution.

THE MOON-FORMING EVENT AND EARTH'S PRIMORDIAL MAGMA OCEAN

Models of early Earth suggest that a combination of thermal inputs from incessant large impacts, the decay of short-lived radioactive elements, and the heat of core formation (Solomon 1979; Wetherill 1990; Tonks and Melosh 1993; Righter and Drake 1999; Elkins-Tanton 2008, 2012; Lebrun et al. 2013; Tucker and Mukhopadhyay 2014), as well as significant tidal heating following the Moon's formation (Zahnle et al.2007) and the blanketing effects of a dense early atmosphere (Matsui and Abe 1986), may have led to multiple regional magma lake or global magma ocean events. Here we focus primarily on mineralogical consequences during the first tens of million years following the Moon-forming event, which was the largest of these postulated major disruptions.

Scenarios for the Moon's origin rely on the catastrophic collision between proto-Earth and a smaller planet-sized body at > 4.4 Ga (Stevenson 1987; Canup and Asphaug 2001; Cuk and Stewart 2012; Barr 2016; Young et al. 2016; Barboni et al. 2017; Thiemens et al. 2018). The timing of this event is a matter of considerable debate. Barboni et al. (2017) propose that Moon formation occurred at ~ 4.51 Ga, based primarily on U-Pb and Hf isotopic systematics. However, the absence of variations in lunar $^{182}W/^{184}W$ attributable to the decay of short-lived ^{182}Hf suggest that this age is an upper limit (R. Carlson, personal communications, 29 September 2021). Other researchers favor a significantly younger Moon, with the lower age limit constrained by the oldest known zircon grains at ~4.37 Ga (Valley et al. 2014). For example, Carlson et al. (2014) and Borg et al. (2015) cite the predonderance of lunar crustal ages < 4.39 Ga as evidence for an origin event close to 4.4 Ga – results that are amplified by estimates of the age of a lunar magma ocean (Borg et al. 2019). Rather than assuming a specific age for the Moon's formation, we consider a range of possible dates: 4.45 +/- 0.06 Ga. Our analysis, therefore, focuses on plausible terrestrial minerals formed prior to the oldest known zircon grain.

Whatever the exact age of the Moon, the lunar origin event temporarily destroyed Earth's crustal mineralogy. A leading hypothesis for the Moon's formation invokes a high-energy, high-angular-momentum impact of a Mars-sized object and subsequent formation of a synestia – an energetic, planetary-scale structure of vaporized material that exceeded Earth's corotation limit, thus ultimately forming one or more companion bodies (Lock et al. 2018, 2020). Such a violent scenario is consistent with some models of Earth-Moon orbital dynamics, while explaining similarities in the chemical and isotopic compositions of the two bodies. In all collisional models, the Moon-forming impact obliterated all traces of Earth's prior near-surface mineralogy.

The uncertain crystallization history of Earth's magma ocean can be understood in part by observations and modeling of well-preserved vestiges of the Moon's compositionally similar magma ocean. Most models of lunar magma ocean cooling and solidification favor an initial period of equilibrium crystallization, owing to inefficient crystal-liquid separation in a turbulent convecting magma body (Tonks and Melosh 1990; Snyder et al. 1992; Elardo et al. 2011). This interval of equilibrium crystallization was followed by gravitationally-driven formation of concentric cumulate layers and consequent chemical fractionation. Denser Mg-rich olivine cumulates, then olivine plus Mg-rich orthopyroxene crystals, sank to the base of the magma ocean, with corresponding enrichment of the residual magma ocean in Ca, Fe, Al, Ti, Si, and a number of minor elements (Tonks and Melosh 1990; Longhi et al. 2010; Elkins-Tanton et al. 2011; Lin et al. 2017). As cooling and solidification progressed, less dense calcic plagioclase crystallized and floated to form the anorthositic mountains of the lunar highlands (Wood et al. 1970; Warren et al. 1983; Norman et al. 2003; Arai and Maruyama 2017). In all viable lunar models, later stages of fractional crystallization of the residual magma ocean resulted in divergent compositions, including the crustal accumulation of KREEP basalt [i.e., enriched in

147 potassium (K), rare earth elements (REE), and phosphorus (P)] and localized silicic lithologies
148 (Warren et al. 1983; Chevrel et al. 1999; Wieczorek and Zuber 2001; Jolliff et al. 2006, 2011;
149 Yamamoto et al. 2012).

150 The evolution of Earth's magma ocean may have paralleled that of the Moon in its broad
151 outlines, but important differences prevailed as a consequence of the contrasting sizes and
152 associated pressure effects of Earth and Moon, coupled with their differing volatile
153 compositions. In particular, while the Moon is not completely dry (Saal et al. 2008; Hui et al.
154 2013), the average water content of lunar magmas (a few hundred ppm) was likely at least an
155 order of magnitude less than that of Hadean terrestrial magmas (e.g., Moore 1970; Kuritani et al.
156 2014) owing to early escape of volatiles from the Moon's weaker gravitational field. In addition,
157 magma ocean pressures in the Moon did not exceed 4 GPa, which is an order of magnitude less
158 than that of Earth's postulated magma ocean (e.g., Deng et al. 2020).

159 Competing models for Earth's magma ocean solidification differ in significant ways. Some
160 hypotheses favor a prolonged period of equilibrium crystallization in a dynamically convecting
161 mantle (Solomatov et al. 1993; Solomatov and Stephenson 1993a, 1993b, 1993c). Other
162 scenarios suggest that Earth's mantle developed mineralogical and compositional stratification
163 early in the solidification process (Abe 1993, 1997; Pilchin and Eppelbaum 2012), perhaps as a
164 consequence of a Hadean "stagnant lid" (O'Neill and Debaille 2014; Ernst et al. 2016), which for
165 a time would have significantly reduced mantle convection. Such an early stratification could
166 help to explain the observed nonchondritic distribution of isotopes derived from short-lived
167 radioactive isotopes (Boyet and Carlson 2005, 2006; O'Neil et al. 2008; Brown et al. 2014).
168 Subsequently, gravitationally unstable cumulates of mantle silicate minerals may have

overturned to form more stable layered configurations that were resistant to the onset of large-scale thermal convection (Elkins-Tanton 2008, 2012; Schaefer and Elkins-Tanton 2018).

The timing of magma ocean solidification was probably rapid in the context of Hadean chronology, perhaps no more than a few million years (Abe 1997; Solomatov 2000, 2007), though rates of planetary cooling were highly dependent on atmospheric composition and density (Lebrun et al. 2013). Elkins-Tanton (2008) calculates that 98% of mantle magma ocean solidification occurred within 5 million years under most postulated initial conditions of atmosphere and volatile composition, with clement surface conditions developing within a few tens of millions of years. Such a short solidification interval points to the possibility of repeated magma lake or ocean events following a sequence of large (> 100 km diameter) impacts over hundreds of millions of years (Marchi et al. 2014; Evans et al. 2018).

EARTH'S EARLIEST CRUSTAL MINERALOGY

A central objective of this contribution is to suggest a plausible mineralogy of Earth's earliest crust, prior to 4.37 Ga. In this regard, the details of magma ocean crystallization in Earth's mantle, such as the extent of large-scale stratification, crystal settling, chemical fractionation, and mantle overturn, may not be critical. Even details of the bulk composition of Earth, for example whether it was close to chondritic or some fractionated variant (Caro et al. 2003; Caro and Bourdon 2010; DePaolo 2013), is likely of secondary importance to estimates of early Hadean crustal mineralogy. Mafic lithologies (i.e., basalt and gabbro) and their primary minerals would have dominated any plausible stable near-surface scenario, while late-stage residual magmatic fluids enriched in incompatible elements inevitably led to a modest degree of mineralogical diversity.

This is the peer-reviewed, final accepted version for American Mineralogist, published by the Mineralogical Society of America.
The published version is subject to change. Cite as Authors (Year) Title. American Mineralogist, in press.
DOI: https://doi.org/10.2138/am-2022-8329. http://www.minsocam.org/

In developing our list of Earth's earliest minerals, we have made four assumptions about the near-surface Hadean world:

(1) Most near-surface primary mineralization was the consequence of widespread volcanic activity and associated intrusive rocks.

(2) A significant fraction of Earth's surface (far more than today's world) was covered by a globe-spanning water ocean prior to 4.37 Ga.

(3) Some volcanic terrains breached the ocean surface, resulting in significant areas of dry land (though far less than today's world).

(4) A dynamic atmosphere rich in CO_2 and H_2O featured rain, lightning, and other surface interactions.

The resulting hypothetical inventory of 262 early Hadean minerals (Supplementary Table 1 and associated Read-Me file) is based on two principal criteria. First, we look to asteroidal mineralogy preserved in stony achondrite meteorites, which provide an informative baseline. Primary mafic and ultramafic igneous minerals and their thermal, aqueous, and shock alteration products in achondrites point to 114 likely early Hadean minerals in Earth's crust (Morrison and Hazen 2021; Hazen and Morrison 2021, 2022).

Of the 262 minerals that we propose formed on the Hadean Earth, 148 mineral species are not yet known from meteorites. These phases were plausibly formed by dynamic processes in Earth's shallow crust, hydrosphere, and atmosphere. We list more than 60 minerals, including 39 not yet found in meteorites, that were associated with volcanoes by condensation at fumaroles, precipitation in zeolite-bearing basalt cavities, and thermal alteration in lava-borne xenoliths. We speculate that aqueous alteration in Earth's shallow crust produced 106 minerals (at least 67 of which have not been identified in meteorites) in hydrothermal veins, at marine and terrestrial

hydrothermal vents and geysers, in zones of serpentinization, and by low-temperature alteration. An additional 110 species (44 appearing for the first time) may have arisen from processes on the terrestrial surface, including authigenesis, freezing of aqueous solutions, impacts, lightning, evaporation, and photo-reactions with sunlight (Table 1).

It is important to note a large number of possible early Hadean minerals that we do not include in this speculative inventory. For example, we do not list mineral species that are (1) not yet known from achondrite meteorites *and* (2) that are relatively rare on Earth today (i.e., minerals known from fewer than 20 localities; https://mindat.org, accessed 6 September 2021). The gyrolite group of phyllosilicates, none of which is known from meteorites, is a case in point. Gyrolite [$NaCa_{16}Si_{23}AlO_{60}(OH)_8 \cdot 14H_2O$] is found in association with basalt-hosted zeolite minerals or hydrothermally altered lithologies in more than 100 localities (https://mindat.org, accessed 16 September 2021) and therefore it is included in our inventory. However, other less common members of the gyrolite group with similar compositions and parageneses, including reyerite [$(Na,K)_2Ca_{14}(Si,Al)_{24}O_{58}(OH)_8 \cdot 6H_2O$], truscottite [$(Ca,Mn)_{14}Si_{24}O_{58}(OH)_8 \cdot 2H_2O$], and tungusite [$Ca_4Fe_2Si_6O_{15}(OH)_6$], are known from fewer than 10 localities and are not included. In addition, our list of the earliest Hadean minerals does not include species with a number of rare elements, including Li, Be, B, Ga, Ge, Se, Rb, Sr, Y, Cd, Tl, Pb, and U. These criteria reflect the relatively restricted physical and/or chemical conditions of formation that are typical of many rare mineral species (Hazen and Ausubel 2016)—conditions we suggest that were not present on Earth prior to 4.37 Ga.

We do not include minerals known exclusively or primarily from exotic achondrite lithologies (Hazen and Morrison 2021; Morrison and Hazen 2021; Rubin and Ma 2021), including highly

237 reduced phases in enstatite chondrites [e.g., daubréelite ($FeCr_2S_4$); oldhamite (CaS); wasonite
238 (WS)]; rare phosphates and other minerals found as meteorite phases exclusively in angrites
239 [e.g., celsian ($BaAl_2Si_2O_8$); kirschteinite ($CaFeSiO_4$); kuratite ($Ca_2Fe_5TiO_2Si_4Al_2O_{18}$);
240 matyhite [$Ca_9(Ca_{0.5}\square_{0.5})Fe(PO_4)_7$]; tsangpoite [$Ca_5(PO_4)_2(SiO_4)$]; or achondrite phases found
241 only in urelites [eskolaite (Cr_2O_3); suessite (Fe_3Si)]. Similarly, we omit rare minerals in silicate
242 inclusions in iron meteorites [armalcolite [$(Mg,Fe)Ti_2O_5$]; kaersutite
243 ($NaCa_2Mg_3AlTiSi_6Al_2O_{24}$); yagiite ($NaMg_2AlMg_2Si_{12}O_{30}$)]; phases known only as alteration
244 products of calcium-aluminum inclusions [goldmanite ($Ca_3V_2SiAl_2O_{12}$); hutcheonite
245 ($Ca_3Ti_2SiAl_2O_{12}$)]; or any of more than a dozen rare oxides and silicates known only from the
246 Allende CV chondrite [Hazen and Morrison 2021; Rubin and Ma 2021; e.g., adrianite
247 ($Ca_{12}Al_4Mg_3Si_7O_{32}Cl_6$); beckettite ($Ca_2V_6Al_6O_{20}$); chihuahuaite [$(Fe,Mg)Al_{12}O_{19}$];
248 coulsonite [$(Fe,Mg)V_2O_4$)], wadalite ($Ca_6Al_5Si_2O_{16}Cl_3$)].

249 With the exception of 14 plausible sanidinite facies minerals found in thermally
250 metamorphosed xenoliths of mafic and ultramafic lithologies, we do not include metamorphic
251 minerals, such as those known exclusively from regional metamorphic or skarn/contact
252 metamorphic deposits. Thus, for example, minerals of the aenigmatite, osumillite, pumpellyite,
253 scapolite, or vesuvianite groups are not represented in our earliest terrestrial inventory. Such
254 phases require the formation of parent lithologies, then burial (in some instances by subduction)
255 and alteration of those rocks, and subsequent uplift and near-surface exposure (Philpotts and
256 Ague 2009; Brown 2013). While it is plausible that such mineral-forming sequences occurred

early in Earth's history, we defer listing most metamorphic minerals until later in the Precambrian, when the advent of significant continental formation and orogenesis related to plate tectonics enriched mineral inventories. Of special note in this regard, although localized carbonate minerals likely formed in modest volumes at hot springs and in association with the carbonation of mafic minerals exposed to the early CO_2-rich atmosphere, we do not list the more than 350 minerals associated with contact metamorphism of carbonates and associated skarn deposits (Hazen and Morrison 2022; their Supplementary Table 1).

A distinctive characteristic of Earth's crustal evolution has been the emplacement of highly-evolved igneous lithologies that likely represent multiple stages of crystallization, partial melting, and fractionation. Among these rock types are carbonate-bearing kimberlites and carbonatites; complex granite pegmatites, noteworthy for minerals of rare elements such as B, Be, Li, and REE; peraluminous igneous rocks; and Si-depleted alkali igneous suites (agpaitic lithologies) that are exceptionally enriched in Na and K, with corresponding development of feldspathoid minerals (Johannsen 1932, 1937; London 2008; Philpotts and Ague 2009; Bea et al. 2013; Furnes and Dilek 2017; Marks and Markl 2017; Ackerson et al. 2021). We suggest that the diverse mineral species unique to these distinctive igneous rocks did not first appear until later in the Hadean Eon (Hazen and Morrison 2022). Therefore, they will be considered in a subsequent contribution.

We identify 262 kinds of minerals that plausibly formed within a few tens of millions of years after the Moon-forming event (Supplementary Table 1; see also Supplementary "Read Me" file). Of these minerals, 236 are valid species with names approved by the IMA-CNMNC. However, in 26 instances we employ names that deviate from IMA conventions (indicated by blue highlights in Supplementary Table 1). Four of these of these unapproved minerals, including

This is the peer-reviewed, final accepted version for American Mineralogist, published by the Mineralogical Society of America.
The published version is subject to change. Cite as Authors (Year) Title. American Mineralogist, in press.
DOI: https://doi.org/10.2138/am-2022-8329. http://www.minsocam.org/

280 silica glass, basaltic glass, impact-produced amorphous $CaSiO_3$, and maskelynite (impact
281 plagioclase glass), are non-crystalline phases, while two are as yet poorly characterized and
282 unnamed impact Mg-Fe silicates known only from meteorites (Ma et al. 2019a, 2019b), but
283 likely also present on the perpetually blasted early Hadean surface.

284 In 18 cases we lump two or more closely-related minerals into one mineral "root kind"
285 (Hazen et al. 2022). In some cases, we employ unapproved names for petrologically familiar
286 solid solutions. "Biotite" includes various Fe-bearing dark micas with the general formula
287 $[K(Mg,Fe^{2+})_{3-x}Al_x(Al_{1+x}Si_{3-x}O_{10}(OH)_2]$ (Fleet 2003; his Figure 172). "Chlorite" refers to all
288 Mg-Fe-Al-dominant members of the chlorite group, most commonly clinochlore
289 $[Mg_5Al(AlSi_3O_{10})(OH)_8]$, but possibly extending to chamosite
290 $[(Fe^{2+},Mg,Al,Fe^{3+})_6(Si,Al)_4O_{10}(OH,O)_8]$ and sudoite $[Mg_2Al_3(Si_3Al)O_{10}(OH)_8]$ in some
291 Hadean settings, as well (Deer et al. 2009). We lump greenalite $[(Fe^{2+},Fe^{3+})_{2-3}Si_2O_5(OH)_4]$
292 with cronstedtite $[(Fe^{2+},Fe^{3+})_3(Si,Fe^{3+})_2O_5(OH)_4]$, as both are Fe-dominant trioctahedral
293 serpentine group minerals and they appear to form a continuous solid solution.

294 "Hornblende" encompasses a range of aluminous calcic clinoamphiboles, including members
295 of the tschermakite, hastingsite, and pargasite groups with general formula
296 $[(\square,Na)Ca_2(Mg,Fe^{2+})(Al,Si)_2Si_6O_{22}(OH,O)_2]$ (Deer et al. 1997; their Figure 279). "Melilite"
297 refers to intermediate members of the akermanite $[Ca_2MgSi_2O_7]$-gehlenite $[Ca_2Al_2SiO_7]$ series
298 (Deer et al. 1986; their Figure 137); "plagioclase" denotes intermediate members of the albite
299 $(NaAlSi_3O_8)$-anorthite $(CaAl_2Si_2O_8)$ series (Deer et al. 2001; their Figure 1); and we recognize

This is the peer-reviewed, final accepted version for American Mineralogist, published by the Mineralogical Society of America.
The published version is subject to change. Cite as Authors (Year) Title. American Mineralogist, in press.
DOI: https://doi.org/10.2138/am-2022-8329. http://www.minsocam.org/

300 the intimate exsolution of K- and Na-rich alkali feldspars as "perthite." We lump fluorapatite,
301 chlorapatite, and hydroxylapatite into "apatite" [$Ca_5(PO_4)_3(F,Cl,OH)$]; monazite-(Ce), monazite-
302 (La), monazite-(Nd), and monazite-(Sm) into "monazite" [$(REE)(PO_4)$]; and allanite-(Ce),
303 allanite-(La), allanite-(Nd), and allanite-(Y) into "allanite"
304 [$Ca(Y,REE)Ce(Al_2Fe^{2+})(Si_2O_7)(SiO_4)O(OH)$]. Similarly, we use root names for nine zeolite
305 mineral groups: chabazite, clinoptilite, erionite, faujasite, ferrierite, heulandite, levyne,
306 phillipsite, and stilbite (Deer et al. 2004). Finally, in our system we use "orthoenstatite" rather
307 than "enstatite" in order to make a clear distinction from clinoenstatite (all of which are
308 $MgSiO_3$).

309

310 **MINERALOGY OF THE EARLY HADEAN EON (> 4.37 GA): PRIMARY IGNEOUS PHASES**

311 In the following sections we consider 18 terrestrial formational environments for 262
312 plausible early Hadean minerals (Table 1; Supplementary Table 1). In each subsection, the
313 numbers and 3-letter acronyms in parentheses correspond to the 18 numbered rows in Table 1,
314 where they appear in the same order.

315

316 *1. Ultramafic Rocks (UMA):* The initial upper mantle lithologies of Earth's crystallizing magma
317 ocean were ultramafic rocks, defined as igneous rocks composed predominantly of mafic
318 minerals and lacking significant feldspars or feldspathoids (Johannsen 1938; Dick 1989; Isley
319 and Abbott 1999; Guilbert and Park 2007; Philpotts and Ague 2009; Lambart et al. 2016).
320 Intrusive ultramafic rocks include olivine-dominant peridotite and pyroxene-dominant
321 pyroxenite, which are the two major lithologies of Earth's upper mantle. In addition, komatiite is

an Mg-rich ultramafic volcanic rock with a distinctive quench texture of skeletal "spinifex" olivine, clinopyroxene, orthopyroxene, and glass – features that point to olivine as a rapidly crystallized liquidus mineral and thus suggesting a high temperature of eruption (> 1650 ºC), presumably when Earth had a much steeper geothermal gradient than today (Green 1975; Shore and Fowler 1999; Faure et al. 2006).

Ultramafic lithologies played a significant role in the mineralogy of Hadean Earth's upper mantle (Rollinson 2007; Van Kranendonk et al. 2007), though significant uncertainty remains regarding the relative volumes of ultramafic versus mafic rocks (e.g., Korenaga 2021). Dense ultramafic rocks would not have accumulated at Earth's early Hadean surface in any significant volumes. However, entrained xenolithic rock fragments might have been a pervasive feature of the Hadean crust. Therefore, 41 primary ultramafic minerals are included in our inventory (Supplementary Table 1; column UMA).

The most common primary minerals in ultramafic rocks (Johannsen 1938) include forsteritic olivine (Mg_2SiO_4); clinopyroxene, usually Mg-rich augite, but also aegirine-augite and diopside [collectively $(Ca,Na,Mg,Fe^{2+},Fe^{3+})_2Si_2O_6$]; orthopyroxene (typically close to the Mg end member, enstatite); chromite ($Fe^{2+}Cr_2O_4$); magnetite ($Fe^{2+}Fe^{3+}{}_2O_4$); spinel (ideally $MgAl_2O_4$, but often Cr-rich); ilmenite ($Fe^{2+}Ti^{4+}O_3$); and apatite. Accessory phases (Johannsen 1938) include calcic plagioclase; alkali feldspars [albite ($NaAlSi_3O_8$) and orthoclase ($KAlSi_3O_8$)]; feldspathoids, most commonly nepheline ($NaAlSiO_4$)]; zircon ($ZrSiO_4$); perovskite ($CaTiO_3$); rutile (TiO_2); titanite ($CaTiSiO_5$); pyrope ($Mg_3Al_2Si_3O_{12}$); and analcime ($NaAlSi_2O_6{\cdot}H_2O$). Sulfides, including pyrite, pyrrhotite (Fe_7S_8), and pentlandite [$(Ni,Fe)_9S_8$], often associated with

platinum group elements (PGE), are also common accessory minerals in ultramafic rocks, perhaps at times derived from an immiscible S- and PGE-rich fluid (e.g., Maier 2005; Collins et al. 2012). In magmas with significant water content, hydrous biopyriboles such as hornblende, biotite, and phlogopite [$KMg_3AlSi_3O_{10}(OH)_2$] may be primary phases, as well. Note that Hazen and Morrison (2022) catalogued 123 mineral species that have been identified in a variety of Precambrian ultramafic intrusive and extrusive igneous rocks, including some hydrothermally altered phases and associated polymetallic deposits. We suggest that most of those species incorporate rare elements and probably would not have appeared until significantly later in Earth's history.

2. Mafic Rocks (MAF): The dominant Hadean crustal lithologies were plagioclase-bearing mafic rocks, most commonly volcanic basalt and its intrusive equivalent, gabbro (Rollinson 2007; Van Kranendonk et al. 2007; O'Neil et al. 2008). Mafic/ultramafic mineral crusts must have formed at the surface of Earth's magma ocean within a few million years following the synestia (e.g., Elkins-Tanton 2012; Carlson et al. 2015, 2019; O'Neil and Carlson 2017). Earth developed and sustained basaltic crusts as a consequence of adiabatic (decompression) melting of deep mantle cumulates that rose to shallower depths during overturn episodes, probably amplified by impact melting (Elkins-Tanton 2008; Griffin et al. 2014; Carlson et al. 2019). Thus, basaltic volcanism was the initial driver of significant crustal formation. Even so, the relatively cold, dense, and viscous basaltic material likely experienced repeated episodes of foundering that eliminated most vestiges of the first crust (Brown et al. 2014).

Of the several varieties of mafic rocks found on Earth today, only tholeiitic basalts associated with partial melting of depleted mantle lithosphere by mantle plumes are likely to have played a

major role in the early Hadean Eon (e.g., Sharkov and Bogina 2009). By contrast, other mafic lithologies, including alkali basalts and boninities, represent later (though possibly Hadean) partial melts. For example, boninitic magmas, which are relatively enriched in Si and Mg, have been ascribed to a two-stage melting process associated with subduction and are thus of later genesis (Duncan and Green, 1987).

Hazen and Morrison (2022) identified 93 mineral species documented to occur in Precambrian mafic igneous rocks. However, most of those minerals are scarce phases that incorporate one or more rare elements and therefore probably appeared later in the Precambrian. Here we tabulate 39 primary minerals (Supplementary Table 1; column MAF) that likely occurred prior to 4.37 Ga in basalt and gabbro, including calcic plagioclase (usually labradorite or bytownite), clinopyroxene (dominantly augite, but also diopside), orthopyroxene (ranging from Mg-rich enstatite to more Fe-rich bronzite or hypersthene), forsteritic olivine, hornblende, biotite, apatite, magnetite, ilmenite, spinel, and chromite (Johannsen 1937). If present, quartz (SiO_2) and orthoclase were among the last minerals to crystallize. Accessory phases include zircon, pyrope, corundum (Al_2O_3), titanite, and graphite (C), as well as Fe sulfides (pyrite and pyrrhotite). Among the most important solid phases associated with mafic volcanism is basaltic glass. Though not an approved mineral species by the IMA-CNMNC, we recognize basaltic glass as a "mineral natural kind" (Supplementary Table 1).

3. Silica-rich rocks (SIL): An important unanswered question is the age and extent of Earth's earliest Si-rich (i.e., granitic/felsic) lithologies. So-called "TTG" (tonalite–trondhjemite–granodiorite) rocks with quartz and Na-Ca feldspar (though relatively minor K-feldspar), often in association with greenstone belts, represent the dominant lithologies preserved from the

389 Eoarchean Era (Condie and Benn 2006; Hamilton 2007; O'Neil et al. 2011; O'Neill and Debaille
390 2014). The origin of these TTG terranes has been ascribed to partial melting of subducted
391 oceanic basalt crust – a process that would have been enhanced by the elevated early
392 Precambrian geothermal gradient (Martin and Moyen 2002; Martin et al. 2005; Hamilton 2007).
393 However, subduction (and the implication of related plate tectonic processes) is not required for
394 TTG formation. Similar partial melting events could have occurred long before modern-style
395 subduction by the chaotic foundering and subsequent melting of mafic crust (e.g., Hamilton
396 2007) or by impact melting (Grieve et al. 2006). Consequently, we suggest that Si-rich
397 lithologies, including TTG suites and other quartz-normative rocks, would have been an early
398 and pervasive feature of Earth's Hadean crust.

399 Several lines of mineralogical and geochemical evidence have been presented to bolster the
400 idea of Hadean quartz normative rocks. In particular, the discovery of zircon grains from the
401 early Hadean Eon (to 4.38 Ga) has raised the possibility of significant primordial granitic terrains
402 (Valley et al. 2002, 2014; Harrison et al., 2005, 2008). A significant fraction of zircon grains
403 older than 4.3 Ga appear to be derived from silica-rich "granitic" or acidic volcanic rocks
404 (Cavosie et al. 2006; Pietranik et al. 2008; Kemp et al. 2010), though isotopic evidence suggests
405 that some of these zircon specimens derive from intermediate rocks. Indeed, several authors have
406 inferred much earlier (~4.50 Ga; i.e., pre-lunar) felsic crust from geochemical data that may
407 point to significant fractionation of REE and Hf prior to the loss of short-lived isotopes, such as
408 ^{146}Sm (Caro et al. 2003; Harrison 2009).

409 Additional evidence for early Si-rich igneous lithologies comes from the Moon and asteroids.
410 On the Moon, localized Si-rich volcanic terrains appear to represent episodes of basalt partial
411 melting, perhaps related to impact melting (Chevrel et al. 1999; Jolliff et al. 2006, 2011). Similar

412 mineralogical outliers have been associated with the partial melting of planetesimals of
413 carbonaceous and ordinary chondrite compositions, for example by Collinet and Grove (2020),
414 who conducted partial melting experiments on various chondritic meteorites. Taking extra care
415 to retain critical volatile alkali elements, they produced initial (up to ~15 wt %) low-density,
416 high-viscosity melts enriched in silica, alumina, and alkalis. Those experimental results parallel
417 the discovery of rare andesitic meteorites – among the oldest known achondrite meteorites at
418 ~4.565 Ga – that presumably represent primitive igneous planetesimal crusts formed prior to
419 significant alkali loss (Barrat et al. 2021). Such rare andesitic meteorites are interpreted as
420 fragments of thin planetesimal crusts that overlaid the volumetrically dominant mafic mantle
421 lithologies, which compose the vast majority of achondrite meteorites.

422 Analogous minor volumes of highly fractionated, localized melts must have played a role in
423 the near-surface mineralogical diversification of early Earth (Warren 1989; Hickman and
424 VanKranendonk 2012; Carlson et al. 2019). The "Bowen trend" of Si-rich residues (Bowen
425 1928) led to Si-, Al-, and alkali-enriched magmas via 2 to 3% melting of wet peridotitic mantle,
426 which is depleted in alkalis relative to primitive chondrites (Kinzler and Grove 1992; Baker et al.
427 1995). In addition, Miyazaki and Korenaga (2019a, 2019b) suggest that fractional crystallization
428 of a magma ocean resulted in outer layers with mafic minerals relatively enriched in Fe (i.e., the
429 "Fenner fractionation trend;" Fenner 1929). Harrison (2009) amplifies this theme by positing a
430 relatively shallow magma ocean (< 250 km) with forsterite crystallization and settling. The
431 residual Si- and Al-rich melt rises to crustal depths and rapidly nucleates feldspar (Morse 1986),
432 creating a tonalitic, high-viscosity mush that coalesced into "rockbergs of stable, felsic crust."
433 Harrison (2009) suggests that tonalitic crust could have appeared shortly after Earth's formation,

as well as soon after the Moon-forming event – hypotheses consistent with evidence from Hadean zircons (Harrison et al. 2008).

The primary mineralogy of early Hadean quartz normative rocks would have included quartz, plagioclase (typically Na-dominant oligoclase-andesine), orthoclase, microcline ($KAlSi_3O_8$), perthite, muscovite [$KAl_2(AlSi_3)O_{10}(OH)_2$], biotite, hornblende, arfvedsonite [$NaNa_2(Fe^{2+}_4Fe^{3+})Si_8O_{22}(OH)_2$], anthopyllite [$\square Mg_7Si_8O_{22}(OH)_2$], almandine ($Fe^{2+}_3Al_2Si_3O_{12}$), orthopyroxene (usually an intermediate Mg-Fe composition, such as hypersthene), clinopyroxene (including augite, diopside, and aegirine-augite), fayalite (Fe_2SiO_4), titanite, magnetite, apatite, zircon, rutile, ilmenite, pyrite, and pyrrhotite (e.g., Johannsen 1932).

In Supplementary Table 1 (column SIL) we tabulate 32 plausible minerals in early Hadean Si-rich rocks. This list is admittedly conservative. For example, we do not list the most common minerals with essential Li [spodumene ($LiAlSi_2O_6$) or Li-rich mica], Be (beryl group), or B (tourmaline group), each of which requires significant local concentration of a rare element (London 2008). Neither do we include such common granitic accessory minerals as cassiterite (SnO_2), molybdenite (MoS_2), or topaz ($Al_2SiO_4F_2$)– phases that we suggest first appeared later in the Hadean Eon, based in part on their absence in the Si-rich lithologies of known lunar or meteoritic samples.

4. Anorthosite (ANO): Anorthosites are distinctive igneous rocks composed almost entirely of macrocrystalline plagioclase feldspar. On Earth, most large anorthosite bodies formed during one relatively short, enigmatic interval during the Mesoproterozoic, between ~1.45 to 1.10 Ga

455 (Philpotts and Ague 2009, and references therein). Other calcic (An > 80) megacrystic
456 anorthositic bodies occur as minor lithologies in some greenstone belts of the Archean Eon as
457 early as ~3.7 Ga (Ashwal 2010). However, recent speculations regarding the possibility of
458 extensive anorthosite bodies on early Earth – perhaps even continent-scale anorthositic
459 development, now lost to subduction (Kawai et al. 2009; Maruyama et al. 2013; Maruyama and
460 Ebisuzaki 2017; Dohm et al. 2018; Yoshiya et al. 2018) – deserve comment.

461 Hypotheses related to Hadean terrestrial anorthosites draw analogies to lunar petrology.
462 Abundant anorthosites are among the most ancient rocks on the Moon, where these relatively
463 low-density rocks rose diapirically to form the lunar highlands. Evidently, plagioclase
464 crystallized in a relatively dry, low-pressure magma body and those crystals subsequently floated
465 to the Moon's surface to form extensive cumulates. However, comparisons of Earth and Moon in
466 this regard are flawed. Experimental measurements have shown that plagioclase is initially
467 negatively buoyant at high pressures in the presumed relatively hydrous silicate melts of early
468 Earth's mantle (Condie 1982; Taylor 1982; Taylor and McLennan 1985). Plagioclase is buoyant
469 at the relatively shallow depths (tens of kilometers) of its stability in Earth's crust; however, the
470 high fraction of crystals and consequent increased viscosity would render significant plagioclase
471 flotation difficult (Elkins-Tanton 2012). Furthermore, numerous phase equilibria studies
472 demonstrate that basalt/gabbro would have been the dominant residual igneous crustal lithology
473 derived by crystallization of a peridotitic mantle magma (e.g., Yoder 1976, and references
474 therein), minimizing the role of anorthosite in the Hadean crust.

475 We conclude that plagioclase-dominant igneous rocks would have represented a minor
476 component of Earth's early crust. However, all of the primary minerals associated with
477 anorthosite today, including calcic plagioclase, alkali feldspar, clinopyroxene, orthopyroxene,

478 forsterite, hornblende, biotite, zircon, titanite, magnetite, ilmenite, rutile, garnet, and pyrite
479 (Johannsen 1937), are also present in the mineral inventories of other probable Hadean igneous
480 minerals (Supplementary Table 1; column ANO). Therefore, the presence or absence of
481 anorthosite does not significantly alter the conclusions of this compilation.
482
483 *5. Volcanic fumarole minerals (FUM):* In addition to the primary igneous minerals outlined
484 above, three other processes related to volcanism may have added to early Earth's mineral
485 diversity. Today, volcanic fumaroles and mariolitic cavities host a remarkable variety of more
486 than 400 minerals that condense directly from hot vapors (Grapes 2006; Vergasova and Filatov
487 2016; Hazen and Morrison 2022). Of these species, we ascribe only 23 fumarolic minerals that
488 incorporate relatively common elements to the earliest episodes of Hadean volcanism
489 (Supplementary Table 1; column FUM). Five of these phases are silicates [albite, cristobalite
490 (SiO_2), fluorophlogopite, sanidine ($KAlSi_3O_8$), and tridymite (SiO_2)], one is the halide fluorite
491 (CaF_2), two are native elements (iron and sulphur), and the remaining 10 are sulfides known to
492 be common in modern fumaroles with reduced S-rich vapors [bismuthinite (Bi_2S_3), chalcopyrite
493 ($CuFeS_2$), digenite ($Cu_{1.8}S$), galena (PbS), greenockite (CdS), marcasite (FeS_2), orpiment
494 (As_2S_3), pyrite, realgar (AsS), and wurtzite (ZnS)].
495
496 *6. Basalt-hosted zeolites and other vesicle-filling minerals (ZEO):* A prominent mineralogical
497 feature of many basaltic formations is the extensive development of zeolites and other minerals
498 that precipitated from warm to hot fluids in vesicles. More than 80 zeolite minerals, most of them
499 rare, have been identified (Deer et al. 2004; https://rruff.info/ima, accessed 6 September 2021).

We include 27 vesicle-deposited minerals, including 19 of the most common basalt-hosted zeolite minerals or mineral groups (Supplementary Table 1; column ZEO). For example, we list analcime, chabazite, faujasite, heulandite, laumontite, natrolite, phillipsite, stilbite, and thompsonite, as possible early Hadean minerals. Other plausible ancient minerals deposited in basalt cavities include aragonite and calcite (both $CaCO_3$), gyrolite, and prehnite $[Ca_2Al(Si_3Al)O_{10}(OH)_2]$.

MINERALOGICAL CONSEQUENCES OF THE EARLY ATMOSPHERE AND OCEANS

The diversity of early Earth's near-surface mineralogy must have been dramatically enriched by events related to the formation of the atmosphere and oceans. Hazen and Morrison (2022) cataloged 350 mineral species associated with a variety of plausible Hadean fluid-rock interactions, including subsurface hydrothermal deposits, serpentinization, hot springs and geysers, seafloor hydrothermal vents, low-temperature aqueous alteration, marine authigenesis, evaporite formation, and freezing. Here, we consider a subset of those minerals that may have formed within a few tens of millions of years of the Moon-forming event.

As with all near-surface minerals formed prior to ~4.50 Ga, any vestiges of Earth's pre-lunar atmosphere or oceans were lost in the Moon-forming event. What, then, was the nature and timing of the transition from the incandescent, silicate-rich synestia to a clement planet with persistent atmosphere and oceans? Answers depend in large measure on the initial fractionation and cycling of volatile elements and molecules among several evolving reservoirs, including the convecting and cooling magma ocean, primary minerals of mafic and ultramafic rocks, condensed aqueous fluids in a variety of near-surface environments, and the enveloping gas phases of the atmosphere (e.g., Ikoma et al. 2018).

523 According to some models, the post-lunar magma ocean was largely devolatilized, thus
524 transferring most H_2O, CO_2, alkali metals, and other volatile elements/molecules to the near-
525 surface environment (Zahnle et al. 2010). Even so, some water must have persisted in the mantle,
526 for example as H in nominally anhydrous minerals (Bell and Rossman 1992; Bolfan-Casanova
527 and Keppler 2000; Kohn and Grant 2006; Tikoo and Elkins-Tanton 2017). After the synestia,
528 additional volatiles would have been delivered to Earth's surface by a steady influx of asteroids
529 and comets (e.g., Albarède 2009; Alexander et al. 2012). However, the relative importance of
530 Earth's original volatile budget versus subsequent contributions through post-lunar bombardment
531 remains a matter of debate (Kasting and Howard 2006; Zahnle et al. 2010, 2020).

532 Widely cited models of the early atmosphere posit a dense mixture primarily of CO_2 and
533 H_2O, with N_2, H_2, CO, CH_4, and H_2S, perhaps with a surface pressure greater than 100
534 atmospheres (Zahnle et al. 2010; Pilchin and Eppelbaum 2012). An added wrinkle is speculation
535 that intense post-lunar bombardment of Earth by Fe-Ni metal-bearing inner solar system objects
536 might have generated a correspondingly reduced atmosphere enriched in H_2, CH_4, and NH_3, and
537 thus conducive to some models of organic chemical reactions as prelude to the origins of life
538 (Sekine et al. 2003; Zahnle et al. 2020). However, such alteration of the atmosphere by
539 bombardment may have significantly post-dated 4.37 Ga (Evans et al. 2018; Morbidelli et al.
540 2018). In any event, a dense early atmosphere would have led to consequential near-surface
541 feedbacks. For example, water can be very soluble in silicate magmas, which can affect
542 atmospheric composition by H_2O drawdown (Schaefer and Fegley 2010).

Similarly, atmospheric CO_2 readily reacts with mafic minerals to form carbonates, as observed in modern-day ophiolite terrains (Sleep and Zahnle 2001; Kelemen and Matter 2008; Streit et al. 2012; Chavagnac et al. 2013; Shibuya et al. 2013; Giampouras et al. 2020; Kadoya et al. 2020). Incorporation of volatiles by near-surface rocks and magma, coupled with active convection and overturn, could have significantly increased water contents of the crust and upper mantle, ultimately leading to volcanic venting of volatiles rich in H, C, O, N, and S (Gaillard and Scaillet 2014). Even though the initial surface environment of the cooling magma ocean was too hot for the accumulation of liquid water, the primary igneous minerals outlined in sections above would have been subject to alteration by interactions with steam and/or supercritical H_2O- and CO_2-bearing fluids (Zahnle et al. 1988). Therefore, we adopt the view that Hadean Earth developed an active hydrosphere, perhaps within a few million years following the synestia (Wilde et al. 2001; Mojzsis et al. 2001; Harrison 2009; Elkins-Tanton 2011).

Many uncertainties remain regarding Earth's earliest water cycle. For example, the water content of volcanic exhalations (and hence the rate of cycling through the mantle) may have been strongly dependent on atmospheric pressure. Gaillard and Scaillet (2014) suggest that at surface pressure >> 1 atm, as is postulated for Earth soon after the Moon's formation, volcanic emissions are N_2- and CO_2-rich, but relatively dry. By contrast, at ~1 atm volcanic gases are dominated by H_2O, whereas surface pressures << 1 atm favor sulfur-rich gases. If Earth's earliest atmosphere was in excess of 100 bars, then an active surface hydrological cycle may have been delayed.

Ultimately, surface cooling below 100 ºC would have supported condensation of water, resulting in a warm early ocean (Abe and Matsui 1988; Abe 1993; Schaefer and Fegley 2010; Ernst et al. 2016). Models of early Hadean oceans suggest important differences from those of

565 today. For example, Hadean oceans were anoxic and thus likely enriched in soluble reduced ions
566 such as Fe^{2+}, Mn^{2+}, and Co^{2+} compared to today's oceans (Anbar and Knoll 2002; Anbar
567 2008). Dissolved carbon dioxide from a dense CO_2-rich atmosphere may have resulted in
568 initially acidic conditions (Morse and Mackenzie 1998). Early Hadean oceans also probably had
569 significantly higher salinity than modern oceans, both because they were warmer and because
570 Earth's volatile elements (including alkali metals and halogens) were concentrated near the
571 surface after the synestia and before extensive formation of crustal minerals such as alkali
572 feldspars with Na and K (Holland 1984; Knauth 2005; Izawa et al. 2010; Zahnle et al. 2010;
573 Charnay et al. 2017; Marty et al. 2018).
574 The volume and aerial extent of Earth's early oceans are also uncertain. Some researchers
575 point to globe-spanning oceans with perhaps twice today's volume of water, owing to a
576 relatively dry, hot peridotitic mantle prior to subduction-driven cycling of water; with subsequent
577 extensive mantle hydration reduced the amount of surface waters (Jarrard 2003; Korenaga 2008;
578 Korenaga et al. 2017; Kurokawa et al. 2018; Dong et al. 2021; Rosas and Korenaga 2021). If so,
579 then the more voluminous early Hadean oceans would have covered almost all of Earth's surface
580 because of less extreme topography prior to the development of felsic continents and associated
581 orogenesis.
582 We conclude that by 4.37 Ga, lakes and oceans may have covered a significant fraction of
583 Earth's surface (Wilde et al. 2001; Elkins-Tanton 2011; Dong et al. 2021), while the shallow
584 subsurface experienced significant hydrothermal circulation (Heinrich and Henley 1989; Pirajno
585 2009). In the following sections we consider more than 150 plausible minerals that may have
586 formed through fluid-rock interactions prior to 4.37 Ga.
587

This is the peer-reviewed, final accepted version for American Mineralogist, published by the Mineralogical Society of America.
The published version is subject to change. Cite as Authors (Year) Title. American Mineralogist, in press.
DOI: https://doi.org/10.2138/am-2022-8329. http://www.minsocam.org/

588 *7. Hydrothermally deposited subsurface minerals (HYD)*: With more than 850 documented
589 species, subsurface hydrothermal deposits represent one of the most diverse mineral-forming
590 environments on Earth. Hazen and Morrison (2022) identified 129 of those phases, primarily
591 sulfides and a few arsenides of the more common transition metal elements, as well as minerals
592 hosting PGE elements associated with ultramafic lithologies (Mungall and Naldrett 2008), as
593 plausible Hadean species. Here we further reduce that inventory to 54 of the most abundant
594 hydrothermal minerals (i.e., known from 20 or more localities; https://mindat.org, accessed 9
595 September 2021) that might have appeared prior to 4.37 Ga (Supplementary Table 1; column
596 HYD). All of these species are known to be associated with mafic or ultramafic hydrothermal
597 systems and most of them are sulfides or arsenides of Fe, Ni, Cu, Co, or Zn.
598
599 *8. Terrestrial hot springs and geysers (HSG)*: The exposed volcanic surface of the Hadean world,
600 though possibly less extensive than today, would have featured abundant subaerial hot springs
601 and geysers that produced a range of geothermal minerals (Pirajno 2020), perhaps including the
602 earliest terrestrial occurrences of carbonates and sulfates [e.g., anhydrite ($CaSO_4$), aragonite,
603 baryte ($BaSO_4$), calcite, and gypsum ($CaSO_4 \cdot 2H_2O$)]. Widespread low-temperature aqueous
604 alteration of Hadean lithologies would also have enriched early Earth's inventory of hydrous
605 silicates, including clay minerals and zeolites (Deer et al. 2004; Wilson 2013). Supplementary
606 Table 1 (column HSG) lists 30 postulated hot springs and geyser minerals that may have
607 precipitated prior to 4.37 Ga.
608
609 *9. Seafloor hydrothermal vents (SHT)*: Earth's earliest seafloor would have been punctuated by
610 numerous vents that emitted mineral-rich hydrothermal fluids, though the character of vent

chemistry and consequent mineralization may have differed significantly from today. We suspect that compositions would have ranged, as they do today, from sulfide-dominated "black smokers" to carbonate-bearing "white smokers" (Hekinian et al. 1980; Haymon and Kastner 1981; Palandri and Reed 2004; Schwarzenbach and Steele-MacInnis 2020). Accordingly, we list a subset of 32 relatively common minerals, primarily sulfides (19 species), as well as carbonates, sulfates, and hydrous phases that likely occurred in seafloor hydrothermal vent systems (Supplementary Table 1, column SHT).

10. Lava-hosted xenolith minerals (XEN): A modest number of early Hadean minerals were likely formed as a consequence of high-temperature, low-pressure (sanidinite facies) metamorphism of xenoliths, which are varied lithic fragments entrained in a magma (e.g., Grapes 2005). Hazen and Morrison (2022) catalogued 127 plausible Hadean xenolith minerals. However, we suggest that only 14 oxide and silicate species would have been likely to form via sanidinite facies metamorphism of early Hadean ultramafic, mafic, and TTG xenoliths (Supplementary Table 1, column XEN). Furthermore, with the possible exceptions of clinoenstatite and cordierite ($Mg_2Al_4Si_5O_{18}$), all of these minerals also occur in one or more of the igneous rocks already discussed. Note in particular that phases derived from Al-rich sediments [corundum, mullite ($Al_{4+2x}Si_{2-2x}O_{10-x}$; $x \sim 0.4$), sillimanite (Al_2SiO_5)] or by reaction with carbonate xenoliths [gehlenite, larnite (Ca_2SiO_4), wollastonite ($CaSiO_3$)], which are commonly found in recent sanidinite facies metamorphic rocks, are not included in our inventory.

633 *11. Hadean serpentinization (SER)*: The serpentinization of mafic and ultramafic rocks, by which
634 Fe- and Mg-bearing minerals are hydrated in low- to moderate-temperature (to ~400 ºC), near-
635 surface aqueous environments, has been a significant mineral-forming process throughout Earth
636 history (Moody 1976; Russell et al. 2010; Shrenk et al. 2013; Shibuya et al. 2015; Lamadrid et
637 al. 2017; Korenaga 2021; Voosen 2021). Serpentinization played a major role in Earth's crustal
638 evolution by transforming ocean floor mafic and ultramafic rocks to assemblages of serpentine,
639 brucite, magnetite, and dozens of other phases (Blais and Aubrey 1990; Lowell and Rona 2002;
640 Palandri and Reed 2004; Shrenk et al. 2013; Holm et al. 2015; Yoshiya et al. 2018). In
641 Supplementary Table 1 (column SER) we list 46 minerals associated with serpentinization of the
642 primary minerals in near-surface Hadean mafic and ultramafic lithologies (see also Johannsen
643 1938 for lists of common secondary minerals in these rocks). Of these phases, 24 are hydrated
644 Mg-bearing minerals and 18 contain Fe and/or Ni.
645
646 *12. Low-temperature aqueous alteration (LTA)*: In addition to the diverse minerals formed by
647 serpentinization and by precipitation associated with hydrothermal systems, submarine vents, hot
648 springs, and geysers, relatively low-temperature (< 100 ºC) aqueous alteration of Hadean mafic
649 and ultramafic lithologies in subaerial and shallow subsurface environments may have produced
650 scores of mineral species, most notably hydroxides, zeolites, clay minerals, and other hydrous
651 silicates (Deer et al. 2004; Wilson 2013). In Supplementary Table 1 (column LTA) we catalog
652 67 plausible aqueous alteration phases from Earth's first 100 million years. Note that these
653 phases in part mirror minerals found in achondrite meteorites that have experienced aqueous
654 alteration – 22 species are common to both environments (Hazen and Morrison 2021a).
655

This is the peer-reviewed, final accepted version for American Mineralogist, published by the Mineralogical Society of America.
The published version is subject to change. Cite as Authors (Year) Title. American Mineralogist, in press.
DOI: https://doi.org/10.2138/am-2022-8329. http://www.minsocam.org/

13. Marine authigenic minerals (AUT): Interactions of early Hadean seawater with serpentinized rocks and seafloor sediments likely produced an assemblage of authigenic phases, defined as minerals formed *in situ* as a consequence of direct precipitation from an aqueous solution, as opposed to aqueous alteration of prior minerals (see above), for example as a carbonate cement in detrital sediments. Following the conventions of Hazen and Morrison (2022), authigenesis refers only to formation of minerals in low-T (< 100 ºC) shallow sedimentary or porous near-surface environments. We list 39 possible authigenic minerals (Supplementary Table 1; column AUT), most of which are zeolites, clays, or other hydrous phases.

14. Minerals formed by freezing (ICE): The timing of Earth's earliest polar ice caps is unknown, but localized episodes of freezing may have occurred, especially if Earth's axial inclination was episodically greater than today. If so, then as many as three additional mineral species - ice (H_2O), hydrohalite ($NaCl{\cdot}2H_2O$), and ikaite ($CaCO_3{\cdot}6H_2O$) – may have occurred in cold regions (Aquioano et al. 2021; Supplementary Table 1; column ICE).

OTHER MINERAL-FORMING PROCESSES

At least four additional subaerial processes – impacts, lightning, evaporite formation, and photo-oxidation – may have added to early Earth's mineral diversity.

15. Impact mineralization (IMP): Impact mineralization would have been a pervasive feature of the Hadean landscape (e.g., Koeberl 2006). Marchi et al. (2014) proposed a bombardment model of early Earth that suggests repeated reprocessing of most of Earth's surface by large impacts

prior to 4 Ga. They posit, "No substantial large region of the Earth's surface could have survived untouched by impacts and associated outcomes."

Meteorites and terrestrial rocks record shock events with peak transient temperatures and pressures that may have exceeded 3,000 ºC and 100 GPa lasting several seconds (Ohtani et al. 2004; Xie et al. 2006; Tomioka and Miyahara 2017; Stöffler et al 2018, their tables 4 through 11). The mineralogical consequences of such violent events on ultramafic, mafic, and TTG lithologies are well documented through studies of dozens of shocked phases in meteorites and from terrestrial impact craters (Koeberl 2002; Tomioka and Miyahara 2017; Ma 2018; Stöffler et al. 2018; Tschauner 2019; Rubin and Ma 2021). Morrison and Hazen (2021; their Table 2) documented 40 impact minerals known from a range of meteorites. In Supplementary Table 1 (column IMP) we include 41 minerals, of which 36 are also in our inventory of meteorite minerals. Five proposed early Hadean terrestrial impact minerals are not yet known from meteorites: akaogiite (TiO_2; El Goresy et al. 2010), maohokite ($MgFe_2O_4$; Chen et al. 2019), reidite ($ZrSiO_4$; Glass et al. 2002), reisite (TiO_2; Tschauner et al. 2020), and yoshiokaite [$Ca_{1-x}(Al,Si)_2O_4$; Vaniman and Bish 1990]. We do not include impact-generated martensite (α-Fe,Ni) and allabogdanite [$(Fe,Ni)_2P$], as they arise exclusively in iron meteorites. Note also that in 5 instances [akimotoite—hemleyite, $(Mg,Fe)SiO_3$; bridgmanite—hiroseite, $(Mg,Fe)SiO_3$; periclase—wüstite or "magnesiowüstite," (Mg,Fe)O); ringwoodite—ahrensite, $(Mg,Fe)_2SiO_4$; and wadsleyite—asimowite, $(Mg,Fe)_2SiO_4$)] we lump pairs of isostructural species with Mg and Fe end-members because observed shock phases are typically of intermediate compositions (Morrison and Hazen 2021; Hazen et al. 2022).

699 Many of these impact phases are dense high-pressure polymorphs of abundant rock-forming
700 minerals, including olivine, pyroxene, feldspar, and spinel group oxides. The list also includes
701 two shock-induced amorphous phases, silica glass (SiO_2) and the impact plagioclase glass
702 known as maskelynite.
703 An additional mineralogical consequence of large impacts would have been creation of
704 extensive and long-lasting fracture systems that promoted hydrothermal circulation and
705 associated fluid-rock interactions, preferential solution and mobilization of some rare elements,
706 and mineralization (Rodriguez et al. 2005; Pirajno 2009; Osinski et al. 2013).
707
708 *16. Lightning minerals (LIG):* Lightning, which appears to be a pervasive attribute of both
709 terrestrial and gaseous planets with turbulent atmospheres (Williams and Krider 1983; Russell et
710 al. 2008, 2011; Lorenz 2018), is an intriguing and as yet little studied mineral-forming
711 mechanism. In this context, lightning is best known for forming hollow branching structures of
712 fused sediments called fulgurites (Essene and Fisher 1986; Grapes 2006; Pasek et al. 2012).
713 These fascinating objects hold a modest inventory of 9 reported mineral species (Hazen and
714 Morrison 2022), including such reduced phases as graphite, silicon (Si), moissanite (SiC), and
715 schreibersite (Fe_3P). However, we suspect that additional reduced lightning-generated minerals
716 may be associated with strikes on ultramafic and mafic lithologies, notably in association with
717 volcanic lightning (McNutt and Williams 2009; Cimarelli et al. 2014; Van Eaton et al. 2016;
718 Cartier 2020; Smith et al. 2021). Such occurrences may incorporate mineralogical novelties
719 (silicides, phosphides, metal alloys), which may be difficult to detect and recover. For example,
720 the highly-reducing environment generated by the influx of electrons from a lightning strike has
721 been invoked as a possible source of prebiotic reduced P compounds (Pasek and Block 2009;

722 Feng et al. 2021; Hess et al. 2021). Similarly, Ballhaus et al. (2017, 2018a, 2018b, 2021) suggest
723 that enigmatic ultra-reduced phases in ophiolites, including moissanite and a variety of native
724 elements and alloys (e.g., Al, Fe, and Si) may result from lightning strikes, in contrast to Griffin
725 et al. (2016, 2017) and Yang et al. (2018), who argue for a deep-mantle origin of these reduced
726 phases. Similar arguments could be extended to Hadean lightning, especially strikes associated
727 with active volcanoes, and its effects on mafic/ultramafic rocks. Therefore, we list 12 plausible
728 early Hadean lightning-generated minerals (Supplementary Table 1; column LIG).
729
730 *17. Evaporites (EVA):* Evaporite mineralization was an inevitable consequence of land
731 surrounded by a saline ocean. Hazen and Morrison (2022) catalog 210 prebiotic evaporite
732 minerals; however, the great majority of those species are rare borates, halides, sulphates, or
733 carbonates that only appear as a consequence of the evaporation of large stranded saline water
734 bodies or brines after continent-scale landmasses appeared (Holser 1979; Boggs 2006). We list
735 14 plausible early Hadean evaporate minerals, including halides [halite (NaCl); sylvite (KCl);
736 and carnalite ($KMgCl_3 \cdot 6H_2O$)], sulphates [anhydrite; gypsum; kieserite ($MgSO_4 \cdot H_2O$);
737 langbeinite ($K_2Mg_2(SO_4)_3$); kainite ($KMg(SO_4)Cl \cdot 3H_2O$); and polyhalite
738 ($K_2Ca_2Mg(SO_4)_4 \cdot 2H_2O$)], and carbonates [calcite; magnesite ($MgCO_3$)], as recorded in
739 Supplementary Table 1 (see column EVA).
740
741 *18. Minerals formed by photo-reactions (PHO):* A handful of new minerals may have been
742 formed through the effects of sunlight on prior minerals (Kim et al. 2013; Hazen and Morrison
743 2022). For example, pararealgar (As_4S_4) is a common photo-reaction byproduct of realgar,

744 which was a likely early Hadean fumarolic mineral (Roberts et al. 1980). Of special interest are
745 photo-oxidation reactions of reduced Fe^{2+}, Mn^{2+}, and Cu^{1+} minerals, which may have produced
746 Fe^{3+}-, Mn^{3+}-, Mn^{4+}-, and Cu^{2+}-bearing minerals long before the biologically-mediated global
747 oxygenation of the Neoarchean Era. For example, Kim et al. (2013) demonstrated that siderite
748 ($FeCO_3$) in water breaks down to ferric iron oxides [magnetite (Fe_3O_4) or maghemite
749 ($Fe_{2.67}O_4$)] plus H_2 when exposed to ultraviolet light. Similarly, ramsdellite (MnO_2) and
750 digenite ($Cu_{1.8}S$) are possible products of photo-oxidation. In Supplementary Table 1 (column
751 PHO) we list 5 minerals that might have appeared through the action of sunlight on prior species.
752

753 **IMPLICATIONS**

754 *Early Hadean mineralogical parsimony:* This contribution lists 262 minerals that may have
755 emerged on Earth prior to 4.37 Ga via one or more of 18 formation processes. The total of 534
756 combinations of a mineral with a formation process tabulated in Supplementary Table 1
757 represents only 5% of the 10,556 combinations of 5659 mineral species formed by 57 processes
758 recorded by Hazen and Morrison (2022) for Earth today. At least 294 meteorite species, formed
759 by 13 pre-terrestrial processes as detailed in Parts I through V of this series, contributed an
760 additional 455 mineral/formation combinations that would have been present at or near Earth's
761 surface continuously since crustal solidification (Supplementary Table 1). Nevertheless, the
762 diversity of Earth's mineral kingdom has expanded by an order of magnitude since the early
763 Hadean Eon as enhanced fluid-rock interactions, plate tectonics, and biological influences have
764 come into play.

765 Three factors contribute to the relative mineralogical parsimony of early Earth. First, many
766 mineral-forming processes, notably regional metamorphism and other mechanisms associated
767 with plate tectonics, had yet to come into play. Second, more than 40% of known mineral species
768 require concentration of one or more rare chemical elements (Hazen and Morrison 2022); we
769 suggest that much more time was required to achieve these degrees of element selection and
770 localized concentration. Third, approximately 33% of all known mineral species arise
771 exclusively through biological interactions with the environment.

772 Interestingly, the formation mechanisms of minerals that we ascribe to early Earth may
773 closely parallel those of Mars during its first billion years. Like Earth, Mars probably
774 experienced an early magma ocean with subsequent wide-ranging mafic volcanism, as well as
775 minor volumes of Si-, Al-, and alkali-rich partial melts. Mars had a dynamic and extensive
776 hydrosphere, with associated mineralization by hydrothermal deposition, water-rock alteration,
777 authigenesis, and evaporites. And, like Earth, the surface of early Mars was subject to impact
778 mineralization, photo-oxidation, lightning, and freezing, with the addition of the full spectrum of
779 meteorite minerals. Consequently, we suggest that Part VI of the evolutionary system of Earth's
780 mineralogy may provide a baseline for Mars mineralogy, as well.

781

782 *Mineral network analysis:* Network graphs have the potential to reveal relationships among large
783 numbers of minerals and their modes of formation (Morrison et al. 2017). The earliest stages of
784 Earth's mineral evolution are illustrated in Figure 1, which is a bipartite network graph that
785 illustrates relationships among 442 terrestrial and/or meteorite minerals and 31 processes by
786 which those minerals formed. This representation of minerals that would have been found on
787 Earth prior to 4.37 Ga includes 13 mineral-forming processes in meteorites (represented by black

This is the peer-reviewed, final accepted version for American Mineralogist, published by the Mineralogical Society of America.
The published version is subject to change. Cite as Authors (Year) Title. American Mineralogist, in press.
DOI: https://doi.org/10.2138/am-2022-8329. http://www.minsocam.org/

788 icons shaped as a star, disk, cloud, or planet) and 18 mineral-forming processes on early Earth
789 (represented by black icons shaped as a volcano, droplet, planet, lightning, or lightbulb). Mineral
790 nodes appear in three colors: red for 180 meteorite minerals not expected to form on early Earth,
791 green for 148 minerals suspected to form on early Earth but not known from meteorites, and
792 yellow for 114 minerals from both groups.

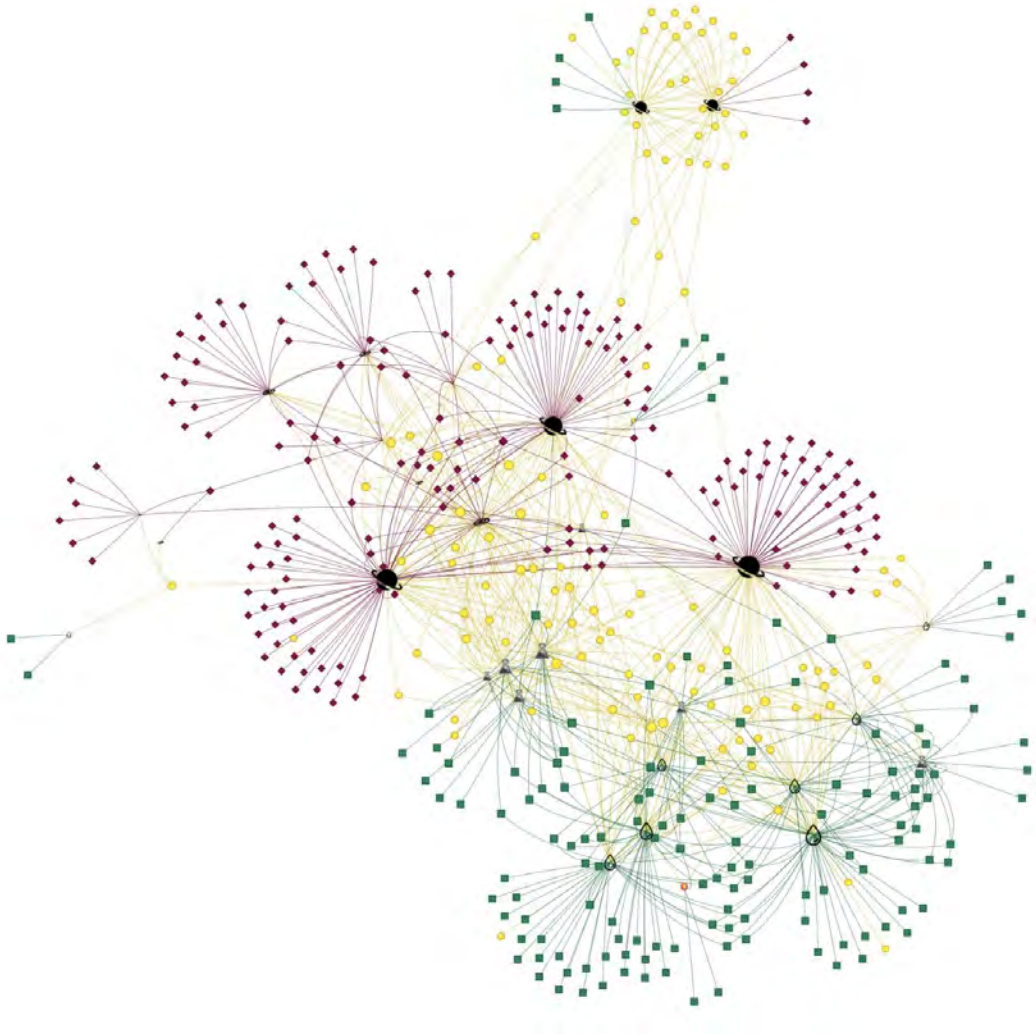

793

794 Figure 1. This bipartite network graph illustrates relationships among 442 different mineral
795 species (represented by square- or diamond-shaped colored nodes) and 31 formation processes of
796 those minerals (represented by various shaped black nodes). The gray lines ("edges") between

these two types of nodes indicate 988 proposed combinations of a mineral species and a mode of formation. Note that each mineral is linked to one or more mode of formation, while each mode of formation is linked to one or more minerals.

This network graph includes 13 nodes representing formation processes associated with meteorites and 18 nodes representing formation processes occurring on early Earth. The 442 minerals include 148 species from early Earth only, represented by green squares; 180 species from meteorites only, represented by red diamonds; and 114 species from both meteorites and early Earth, represented by yellow circles. See Figures 2A through 2D for detailed enlargements of four areas of this graph.

The topology of Figure 1 reflects the diversity of formation environments on early Earth. At the largest scale, minerals formed exclusively on Earth (green nodes) versus those exclusively from meteorites (red nodes) are well separated, with most minerals from both environments creating a yellow band across the middle of the graph. Additional trends are also evident, with clustering of minerals formed by various primary and secondary processes.

Figure 2 focuses on key areas of this network graph. As might be expected, significant overlaps between terrestrial and meteorite minerals occur among some of these various subsets of early Hadean mineralogy. For example, 36 of 41 impact-generated minerals suspected to have occurred on early Earth are also found in meteorites (Figure 2A). Most of these phases are unique to the extremely high-temperature and high-pressure conditions of shock metamorphism. Therefore, nodes representing meteorite and terrestrial impact formation processes lie close to each other at the top of the graph, but significantly separated from most other minerals. Indeed,

This is the peer-reviewed, final accepted version for American Mineralogist, published by the Mineralogical Society of America.
The published version is subject to change. Cite as Authors (Year) Title. American Mineralogist, in press.
DOI: https://doi.org/10.2138/am-2022-8329. http://www.minsocam.org/

819 only five minerals, including diamond (as a stellar condensate), clinoenstatite, and cordierite (in
820 xenoliths), connect impact minerals with other early Earth minerals.

821 **A.**

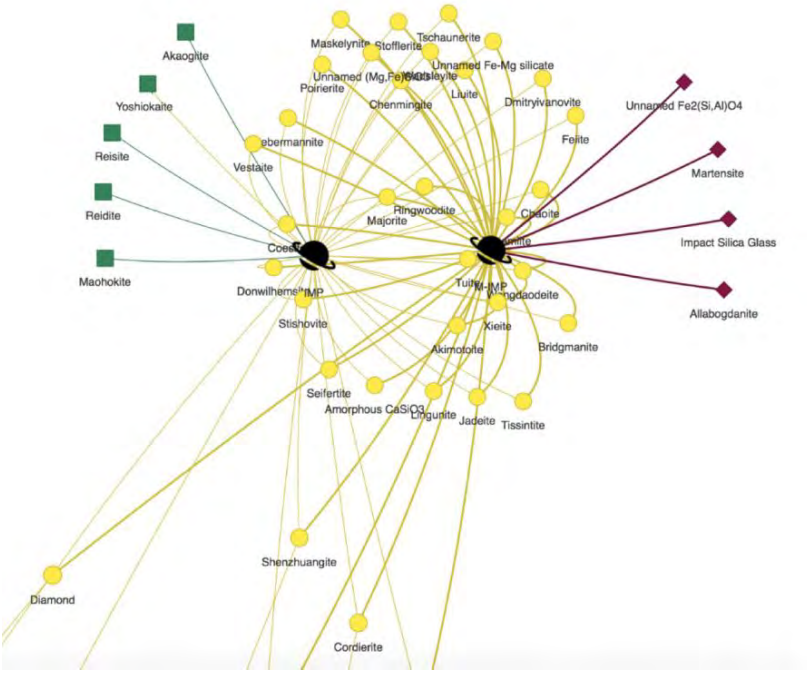

This is the peer-reviewed, final accepted version for American Mineralogist, published by the Mineralogical Society of America.
The published version is subject to change. Cite as Authors (Year) Title. American Mineralogist, in press.
DOI: https://doi.org/10.2138/am-2022-8329. http://www.minsocam.org/

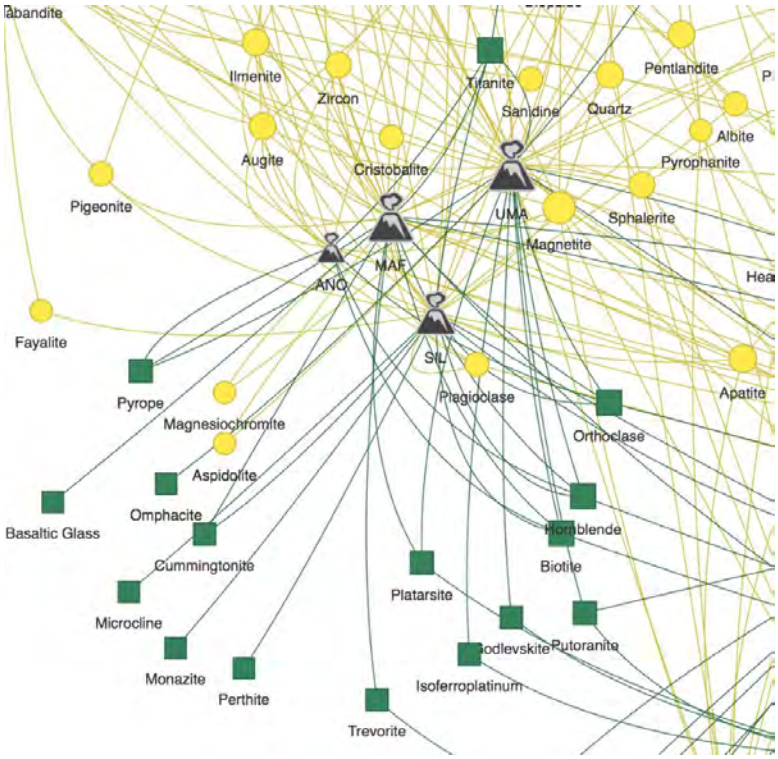

B.

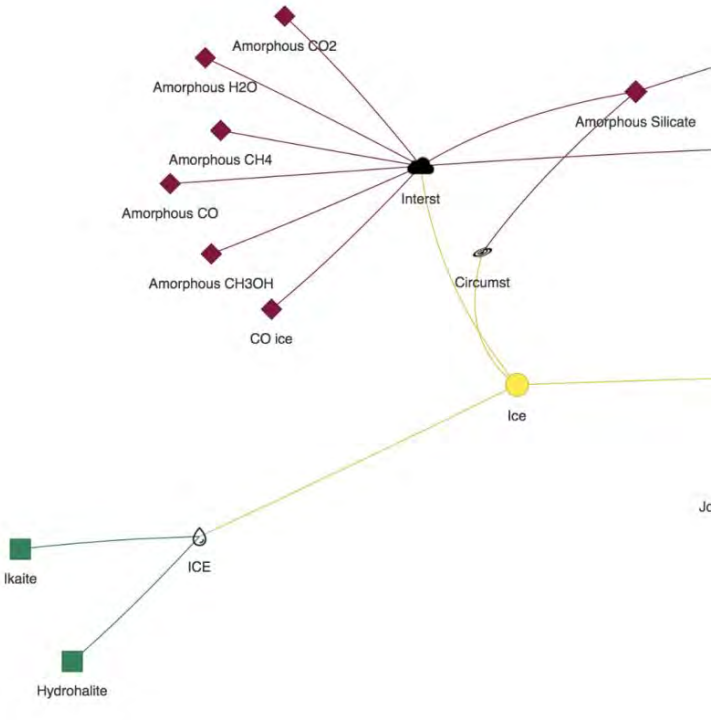

C.

This is the peer-reviewed, final accepted version for American Mineralogist, published by the Mineralogical Society of America.
The published version is subject to change. Cite as Authors (Year) Title. American Mineralogist, in press.
DOI: https://doi.org/10.2138/am-2022-8329. http://www.minsocam.org/

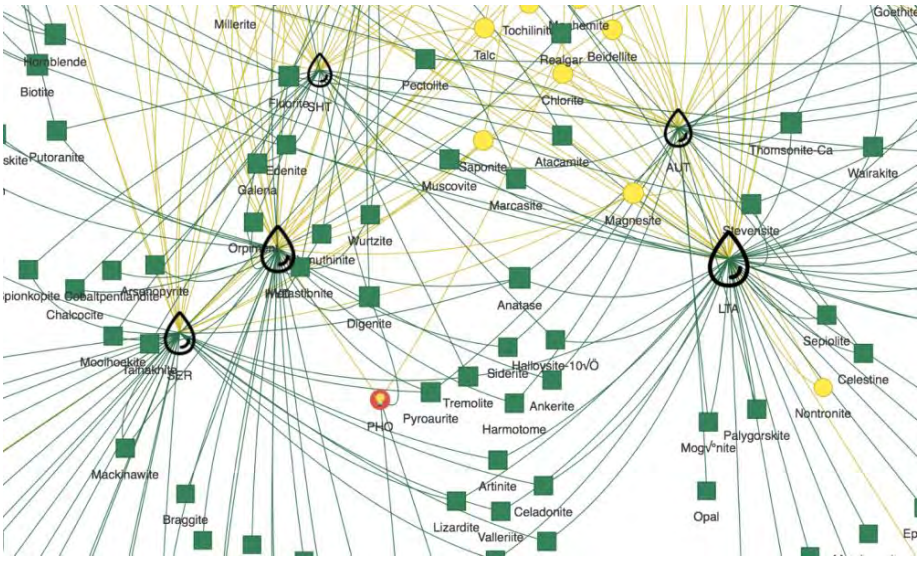

Figure 2. Selected areas of the bipartite network graph (Figure 1).

A. Impact minerals from meteorites (planet-shaped icon on the right) and terrestrial sites (lanet-shaped icon on the left) largely overlap. Five terrestrial impact minerals are predicted to have occurred on early Hadean Earth but have not yet been found in meteorites, whereas four meteorite impact minerals related to shocked iron meteorites are not yet known from terrestrial settings. Only five minerals, including diamond, clinoenstatite, and cordierite, connect these impact phases with the rest of the graph.

B. Primary igneous phases from early Earth, represented by volcano-shaped icons (UMA = ultramafic rocks; MAF = mafic rocks; SIL = quartz normative rocks; ANO = anorthosite), include many phases that are also found in the mafic lithologies of achondrite meteorites, and therefore form a centralized cluster of green and yellow nodes.

C. Low-temperature and low-pressure condensates ("ices") form a distinct cluster of phases in the lower left of the network graph. Water ice provides important connections among interstellar (cloud icon), circumstellar (disk icon), cold asteroidal surface (planet icon), and terrestrial ice (droplet icon) environments.

D. Numerous minerals formed by water-rock interactions on Earth form a distinct cluster of green nodes near the bottom of the graph. The five droplet-shaped icons are separated into two lower-temperature formation processes on the right (AUT = authigenic; LTA = low-temperature alteration) and three higher-temperature processes on the left (SER = serpentinite; HYD =

844 hydrothermal vein; SHT = seafloor hydrothermal vent). Relatively few of these phases are also
845 known from meteorites.
846
847 Significant overlaps occur among many of the minerals that form as primary igneous phases
848 in stony achondrites and that also occur in Earth's ultramafic, mafic, and anorthositic lithologies
849 (Figure 2B). These minerals form a centralized cluster of yellow and green nodes. By contrast,
850 low-temperature and low-pressure condensates ("ices") form a distinct cluster of phases in the
851 lower left-hand side of the network graph (Figure 2C). Water ice provides important connections
852 among interstellar, circumstellar, cold asteroidal surface, and terrestrial ice environments.
853 Another group of minerals forms a distinct cluster of phases formed by water-rock
854 interactions (Figure 2D). These minerals, represented by green nodes near the bottom of the
855 graph, are linked to five droplet icons. These icons are further clustered into two lower-
856 temperature formation processes on the right-hand side of Figure 2D (representing authigenic
857 mineralization and low-temperature alteration) and three higher-temperature processes on the
858 left-hand side (including serpentinization, hydrothermal vein deposition, and seafloor
859 hydrothermal vents). Note that relatively few of these phases are also known from meteorites, so
860 they appear as green nodes that tend to be significantly separated from the more centralized
861 phases that share meteorite and Earth origins (i.e., yellow nodes).
862
863 *Minerals and the origins of life:* The paleomineralogy of the Hadean Eon has attracted
864 significant attention in the context of life's origins, because most biogenesis models posit an
865 origin event prior to 4.0 Ga. A wide variety of minerals have been invoked in origins scenarios,
866 some of them not included in lists of early Hadean species (Hazen 2013). For example, phases
867 with postulated catalytic sites such as borates, molybdates, and phosphates (Ricardo et al. 2004;

Kim et al. 2016; Ziegler et al. 2018) are not in our inventories. Even if our Hadean mineral catalog is too limited, and minerals such as borates or molybdates were in fact present prior to 4.37 Ga, they would have been extremely minor phases with trivial total volumes. Is this lack an impediment to essential origins-of-life chemical processes?

We now realize that any chemical element that may have played a critical role in biology today was abundantly available for prebiotic chemistry in the earliest Hadean Eon, if not as an essential element in a Hadean mineral, then as a trace or minor element in one or more common rock-forming minerals (Morrison et al. 2018; Hazen and Morrison 2021b). For example, boron with an average crustal abundance of 10 parts per million (ppm) is typically present at > 100 ppm in augite. Likewise, phosphorus occurs in concentrations > 1000 ppm in olivine, plagioclase, and basaltic glass. Indeed, a range of biologically essential transition elements, including Co, Ni, Cu, Zn, and Mo, were ubiquitous as trace elements in rock-forming oxides and silicates at concentrations many times their average crustal abundance (Hazen and Morrison 2021b; their Table 2.1). In each of these (and many more) instances, common rock-forming minerals are orders-of-magnitude larger crustal reservoirs of rare elements than any other mineralogical source. We conclude that common Hadean minerals provided a diverse and omnipresent range of potentially catalytic surface sites for biogenesis – a facet of prebiotic chemistry that has yet to be explored.

ACKNOWLEDGMENTS

We are especially grateful to Richard Carlson for valuable discussions and a detailed review of an early version of this contribution. Alexander Evans, Edward Grew, Timothy Grove, Jihua Hao, Peter Kelemen, Craig Manning, Karyn Rogers, Dimitri Sverjensky, Lindy Elkins-Tanton, and Michael Walter provided expert advice on aspects of early Earth petrology and geochemistry. We also thank Associate Editor Steven Simon, and reviewers Kent Condie and George Harlow for their thorough, thoughtful, and constructive reviews.

FUNDING

Studies of mineral evolution and mineral ecology have been supported by the Alfred P. Sloan Foundation, the W. M. Keck Foundation, the John Templeton Foundation, the NASA Astrobiology Institute ENIGMA team, a private foundation, and the Carnegie Institution for Science. Any opinions, findings, or recommendations expressed herein are those of the authors and do not necessarily reflect the views of the National Aeronautics and Space Administration.

REFERENCES

Abe, Y. (1993) Physical state of the very early Earth. Lithos, 30, 522 223–522 235.

Abe, Y. (1997) Thermal and chemical evolution of the terrestrial magma ocean. Physics of Earth and Planetary Interiors, 100, 27–39.

Abe, Y., and Matsui, T. (1988) Evolution of an impact-generated H_2O-CO_2 atmosphere and formation of a hot proto-ocean on Earth. Journal of the Atmospheric Sciences, 45, 3081-3101.

Ackerson, M.R., Trail, D., and Buettner, J. (2021) Emergence of peraluminous crustal magmas and implications for the early Earth. Geochemical Perspectives Letters, 17, 50-54.

Albarède, F. (2009) Volatile accretion history of the terrestrial planets and dynamic implications. Nature. 461, 1227–1233.

Alexander, C.M.O'D., Bowden, R., Fogel, M.L., Howard, K.T., Herd, C.D.K., and Nittler L.R. (2012) The provenances of asteroids, and their contributions to the volatile inventories of the terrestrial planets. Science, 337, 721-723.

Anbar, A.D. (2008) Elements and evolution. Science, 322, 1481-1483.

Anbar, A.D., and Knoll, A.H. (2002) Proterozoic ocean chemistry and evolution: A bioinorganic bridge? Science, 297, 1137-1142.

Anthony, J.W., Bideaux, R.A., Bladh, K.W., and Nichols, M.C. (1990-2003) Handbook of Mineralogy, 6 volumes. Mineral Data Publishing.

Aquioano, D., Bruno, M., Pastero, L., and Ghignone, S. (2021) Growth and equilibrium morphology of hydrohalite ($NaCl{\cdot}2H_2O$) and its epitaxy with hexagonal ice crystals. Journal of Physical Chemistry C, 125, 6923−6932.

Arai, T., and Maruyama, S. (2017) Formation of anorthosite on the Moon through magma ocean fractional crystallization. Geoscience Frontiers, 8, 299-308.

925 Armstrong, J.C., Wells, L.E., and Gonzales, G. (2002) Rummaging through Earth's attic for
926 remains of ancient life. Icarus, 160, 183-196.
927 Ashwal, L.D. (2010) The temporality of anorthosites. Canadian Mineralogist, 48, 711-728.
928 Badro, J., and Walter, M. [Eds.] (2015) The Early Earth: Accretion and Differentiation.
929 American Geophysical Union Geophysical Monograph, 212.
930 Baker, M.B., Hirschmann, M.M., Ghiorso, M.S., and Stolper, E.M. (1995) Compositions of near-
931 solidus peridotite melts from experiments and thermodynamic calculations. Nature, 375, 308–
932 311.
933 Ballhaus, C., Wirth, R., Fonseca, R.O.C., Blanchard, H., Pröll, W., Bragagni, A., and Nagel, T.,
934 Schreiber, A., Dittrich, S., Thome, V., Hezel, D.C., Below, R., and Cieszynski, H. (2017)
935 Ultra-high pressure and ultra-reduced minerals in ophiolites may form by lightning strikes.
936 Geochemical Perspective Letters, 5, 42-46.
937 Ballhaus, C., Fonseca, R.O.C., and Bragagni, A. (2018a) Reply to Comment on "Ultra-high
938 pressure and ultra-reduced minerals in ophiolites may form by lightning strikes" by Griffin et
939 al. (2018): No evidence for transition zone metamorphism in the Luobusa ophiolite.
940 Geochemical Perspectives Letters, 7, 3-4.
941 Ballhaus, C., Blanchard, H., Fonseca, R.O.C., and Bragagni, A. (2018b) Reply 2 to Comment on
942 "Ultra-high pressure and ultra-reduced minerals in ophiolites may form by lightning strikes".
943 Geochemical Perspectives Letters, 8, 8-10.
944 Ballhaus, C., Helmy, H.M., Fonseca, R.O.C., Wirth, R., Schrieber, A., and Jons, N. (2021) Ultra-
945 reduced phases in ophiolites cannot come from Earth's mantle. American Mineralogist, 106,
946 1053-1963.
947 Barboni, M., Boehnke, P., Keller, B., Kohl, I.E., Schoene, B., Young, E.D., and McKeegan, K.D.

(2017) Early formation of the Moon 4.51 billion years ago. Science Advances, 3, e1602365.

Barr, A.C. (2016) On the origin of Earth's Moon. Journal of Geophysical Research: Planets, 121, 1573–1601.

Barrat, J.-A., Chaussidon, M., Yamaguchi, A., Beck, P., Villeneuve, J., Byrne, D.J., Broadley, M.W., and Marty, B. (2021) A 4,565-My-old andesite from an extinct chondritic protoplanet. Proceedings of the National Academy of Sciences, 118, e02619118 (7 p.)

Bea, F., Montero, P., Hayssen, F., Rjimati, E., El Archi, A., and Molina, J.F. (2013) Petrology and geochemistry of 2.46 Ga kalsilite and nepheline syenites from the Awsard Massif, Reguibat Rise, West African Craton. A model for generation of extremely K-rich magmas at the Archean to Proterozoic transition. International Association for Gondwana Research Conference Series, 15, 7-8.

Bell, D., and Rossman, G. (1992) Water in Earth's mantle: the role of nominally anhydrous minerals. Science, 255, 1391–1397.

Bellucci, J.J., Menchin, A.A., Grange, M., Robinson, K.L., Collins, G., Whitehouse, M.J., Snape, J.F., Norman, M.D., and Kring, D.A. (2019) Terrestrial-like zircon in a clast from an Apollo 14 breccia. Earth and Planetary Science Letters, 510, 173-185.

Blais, S., and Auvray, B. (1990) Serpentinization in the Archean komatiitic rocks of the Kuhmo greenstone belt, eastern Finland. Canadian Mineralogist, 28, 55-66.

Boggs, S. (2006) Principles of Sedimentology and Stratigraphy, 4th edition. Pearson Prentice Hall.

Bolfan-Casanova, N., and Keppler, H. (2000) Water partitioning between nominally anhydrous minerals in the MgO-SiO_2-H_2O system up to 24 GPa: implications for the distribution of water in the Earth's mantle. Earth and Planetary Science Letters, 182, 209–221.

971 Borg, L.E., Gaffney, A.M., and Shearer, C.K. (2015) A review of lunar chronology revealing a
972 preponderance of 4.34-4.37 Ga ages. Meteoritics & Planetary Science, 50, 715-732.
973 Borg, L.E., Gaffney, A.M., Kruijer, T.S., Marks, N.A., Sio, C.K., and Wimpenny, J. (2019)
974 Isotopic evidence for a young lunar magma ocean. Earth and Planetary Science Letters, 523,
975 115706 (9 p.).
976 Bowen, N.L. (1928) The Evolution of the Igneous Rocks. Princeton University Press.
977 Bowles, J.F.W., Howie, R.A., Vaughan, D.J., and Zussman, J. (2011) Rock-Forming Minerals.
978 Volume 5A, Second Edition. Non-Silicates: Oxides, Hydroxides and Sulfides. The Geological
979 Society of London.
980 Boyd, R. (1991) Realism, anti-foundationalism and the enthusiasm for natural kinds.
981 Philosophical Studies, 61, 127-148.
982 Boyd, R. (1999) Homeostasis, species, and higher taxa. In: R. Wilson, Ed., Species: New
983 Interdisciplinary Essays, pp.141-186. Cambridge University Press.
984 Boyet, M., and Carlson, R.W. (2005) ^{142}Nd evidence for early (>4.53 billion years ago) global
985 differentiation of the silicate Earth. Science, 309, 576–581.
986 Boyet, M., and Carlson, R.W. (2006) A new geochemical model for the Earth's mantle inferred
987 from ^{146}Sm-^{142}Nd systematics. Earth and Planetary Science Letters, 250, 254–268.
988 Boyet, M., Blichert-Toft, J., Rosing, M., Storey, M., Telouk, P., and Albarède. F. (2003) ^{142}Nd
989 evidence for early Earth differentiation. Earth and Planetary Science Letters, 214, 427–442.
990 Brown, M. (2013) The contribution of metamorphic petrology towards understanding
991 Precambrian lithospheric evolution: The last 30 years in review. International Association for
992 Gondwana Research Conference Series, 15, 16-22.

993 Brown, S., Elkins-Tanton, L.T., and Walker, R. (2014) Effects of magma ocean crystallization
994 and overturn on the development of ^{142}Nd and ^{182}W isotopic heterogeneities in the
995 primordial mantle. Earth and Planetary Science Letters, 408, 319–330.
996 Budde, G., Burkhardt, C., Brennecka, G.A., Fischer-Gödde, M., Kruijer, T.S., and Kleine, T.
997 (2016) Molybdenum isotopic complementarity of chondrules and matrix and the dichotomy of
998 carbonaceous and noncarbonaceous meteorites. Earth and Planetary Science Letters, 454,
999 293-303.
1000 Burke, E.A.J. (2006) The end of CNMMN and CCM—Long live the CNMNC! Elements, 2,
1001 388.
1002 Burkhardt, C., Kleine, T., Oberli, F., Pack, A., Bourdon, B., and Wieler, R. (2011) Molybdenum
1003 isotopic anomalies in meteorites: Constraints on solar nebula evolution and the origin of the
1004 Earth. Earth and Planetary Science Letters, 312, 390-400.
1005 Canup, R.M., and Asphaug, E. (2001) Origin of the Moon in a giant impact near the end of
1006 Earth's formation. Nature, 412, 708–712.
1007 Carlson, R.W., Borg, L.E., Gaffney, A.M., and Boyet, M. (2014) Rb-Sr, Sm-Nd and Lu-Hf
1008 isotope systematics of the lunar Mg-suite: the age of the lunar crust and its relation to the time
1009 of Moon formation. Philosophical Transactions of the Royal Society A, 372, 2103.0246 (21
1010 p.).
1011 Carlson, R.W., Boyet, M., O'Neil, J., Rizo, H., and Walker, R.J. (2015) Early differentiation and
1012 its long-term consequences for Earth evolution. In: Badro, J., and Walter, M. (Eds.), The
1013 Early Earth: Accretion and Differentiation. American Geophysical Union Geophysical
1014 Monograph, 212, 143-172.

1015 Carlson, R.W., Garçon, M., O'Neil, J., Reimink, J., and Rizo, H. (2019) The nature of Earth's
1016 first crust. Chemical Geology, 530, 119321 (25 p.).
1017 Caro, G., and Bourdon, B. (2010) Non-chondritic Sm/Nd ratio in the terrestrial planets:
1018 Consequences for the geochemical evolution of the mantle–crust system. Geochimica et
1019 Cosmochimic Acta, 74, 3333–3349.
1020 Caro, G., Bourdon, B., Birck, J.L., and Moorbath, S. (2003) ^{146}Sm-^{142}Nd evidence from Isua
1021 metamorphosed sediments for early differentiation of the Earth's mantle. Nature, 423, 428–
1022 432.
1023 Cartier, K.M.S. (2020) Planetary lightning: Same physics, distant worlds. Eos, 101.
1024 https://doi.org/10.1029/2020EO142803
1025 Cavosie, A.J., Valley, J.W., Wilde, S.A., and Edinburgh Ion Microprobe Facility (2006)
1026 Correlated microanalysis of zircon: trace element, δ^{18}O and U–Th–Pb isotopic constraints on
1027 the igneous origin of complex > 3900 Ma detrital grains. Geochimica et Cosmochimica Acta,
1028 70, 5601–5616.
1029 Charnay, B., Le Hir, G., Fluteau, F., Forget, F., and Catling, D.C. (2017) A warm or cold early
1030 Earth? New insights from a 3-D climate-carbon model. Earth and Planetary Science Letters,
1031 474, 97-109.
1032 Chavagnac, V., Ceuleneer, G., Monnin, C., Lansac, B., Hoareau, G., and Boulart, C. (2013)
1033 Mineralogical assemblages forming at hyperalkaline warm springs hosted on ultramafic
1034 rocks: a case study of Oman and Ligurian ophiolites. Geochemistry Geophysics Geosystems,
1035 14, 2474–2495.

1036 Chen, M., Shu, J., Xie, X., and Tan, D. (2019) Maohokite, a post-spinel polymorph of $MgFe_2O_4$
1037 in shocked gneiss from the Xiuyan crater in China. Meteoritics & Planetary Science, 54, 495-
1038 502.
1039 Chevrel, S.D., Pinet, P.C., and Head, J.W. III (1999) Gruithuisen domes region: A candidate for
1040 an extended nonmare volcanism unit on the Moon. Journal of Geophysical Research, 104,
1041 16515–16529.
1042 Cimarelli, C., Alatorre-Ibargüengoitia, M.A., Kueppers, U., Scheu, B., and Dingwell, D.B.
1043 (2014) Experimental generation of volcanic lightning. Geology, 42, 79-82.
1044 Cleland, C.E., Hazen, R.M., and Morrison, S.M. (2021) Historical natural kinds in mineralogy:
1045 Systematizing contingency in the context of necessity. Proceedings of the National Academy
1046 of Sciences, 108, e2015370118 (8 p.)
1047 Collinet, M., and Grove, T.L. (2020) Widespread production of silica- and alkali-rich melts at the
1048 onset of planetesimal melting. Geochimica et Cosmochemica Acta, 277, 334-357.
1049 Collins, S.J., Maclennan, J., Pyle, D.M., Barnes, S.-J., and Upton, B.G.J. (2012) Two phases of
1050 sulphide saturation in Réunion magmas: Evidence from cumulates. Earth and Planetary
1051 Science Letters, 337, 104–113.
1052 Condie, K.C. (1982) Plate Tectonics and Crustal Evolution. Pergamon.
1053 Condie, K.C., and Benn, K. (2006) Archean geodynamics: Similar to or different from modern
1054 geodynamics? American Geophysical Union Geophysical Monographs, 164, 47-60.
1055 Crawford, I.A., Baldwin, E.C., Taylor, E.A., Bailey, J.A., and Tsembelis, K. (2008) On the
1056 survivability and detectability of terrestrial meteorites on the Moon. Astrobiology, 8, 242-252.
1057 Cuk, M., and Stewart, S.T. (2012) Making the Moon from a fast-spinning Earth: A giant impact
1058 followed by resonant despinning. Science, 338, 1047-1052.

1059 Deer, W.A., Howie, R.A., and Zussman, J. (1982-2013) Rock-Forming Minerals. Second
1060 Edition. 11 volumes. John Wiley and The Geological Society of London.
1061 Deer, W.A., Howie, R.A., and Zussman, J. (1986) Rock-Forming Minerals. Volume 1B, Second
1062 Edition. Disilicates and Ring Silicates. John Wiley.
1063 Deer, W.A., Howie, R.A., and Zussman, J. (1997) Rock-Forming Minerals. Volume 2B, Second
1064 Edition. Double-Chain Silicates. The Geological Society of London.
1065 Deer, W.A., Howie, R.A., and Zussman, J. (2001) Rock-Forming Minerals. Volume 4A, Second
1066 Edition. Framework Silicates: Feldspars. The Geological Society of London.
1067 Deer, W.A., Howie, R.A., Wise, W.S., and Zussman, J. (2004) Rock-Forming Minerals. Volume
1068 4B, Second Edition. Framework Silicates: Silica Minerals, Feldspathoids and the Zeolites.
1069 The Geological Society of London.
1070 Deer, W.A., Howie, R.A., and Zussman, J. (2009) Rock-Forming Minerals. Volume 3B, Second
1071 Edition. Layered Silicates Excluding Micas and Clay Minerals. The Geological Society of
1072 London.
1073 Deng, J., Du, Z., Karki, B.B., Ghosh, D.B., and Lee, K.K.M. (2020) A magma ocean origin to
1074 divergent redox evolutions of rocky planetary bodies and early atmospheres. Nature
1075 Communications, 11, (7 p.), https://doi.org/10.1038/s41467-020-15757-0.
1076 DePaolo, D.J. (2013) Implications, complications, and simplifications associated with a non-
1077 chondritic early Earth. International Association for Gondwana Research Conference Series,
1078 15, 34-35.
1079 Desch, S.J., Kalyaan, A., and Alexander, C.M.O'D. (2018) The effect of Jupiter's formation on
1080 the distribution of refractory elements and inclusions in meteorites. The Astrophysical Journal
1081 Supplement Series, 238, 11 (31 pp).

1082 Dick, H.J.B. (1989) Abyssal peridotites, very slow spreading ridges and ocean ridge
1083 magmatism. Geological Society of London, Special Publications, 42, 71–105.
1084 Dohm, J.M., Maruyama, S., Kido, M., and Baker, V.R. (2018) A possible anorthositic continent
1085 of early Mars and the role of planetary size for the inception of Earth-like life. Geoscience
1086 Frontiers, 9, 1085-1098.
1087 Dong, J., Fischer, R.A., Stixrude, L.P., and Lithgow-Bertelloni, C.R. (2021) Constraining the
1088 volume of Earth's early oceans with a temperature-dependent mantle water storage capacity
1089 model. AGU Advances, 2, e2020AV000323.
1090 Duncan, R.A., and Green, D.H. (1987) The genesis of refractory melts in the formation of
1091 oceanic crust. Contributions to Mineralogy and Petrology, 96, 326-342.
1092 Elardo, S.M., Draper, D.S., and Shearer, C.K. Jr. (2011) Lunar magma ocean crystallization
1093 revisited: Bulk composition, early cumulate mineralogy, and the source regions of the
1094 highlands Mg-suite. Geochimica et Cosmochimica Acta, 75, 3024-3045.
1095 El Goresy, A., Dubrovinsky, L., Gillet, P., Graup, G., and Chen, M. (2010) Akaogiite: An ultra-
1096 dense polymorph of TiO_2 with the baddeleyite-type structure, in shocked garnet gneiss from
1097 the Ries Crater, Germany. American Mineralogist, 95, 892-895.
1098 Elkins-Tanton, L.T. (2008) Linked magma ocean solidification and atmospheric growth for Earth
1099 and Mars. Earth and Planetary Science Letters, 271, 181-191.
1100 Elkins-Tanton, L.T. (2011) Formation of early water oceans on rocky planets. Astrophysics and
1101 Space Science, 332, 359–364.
1102 Elkins-Tanton, L.T. (2012) Magma oceans in the inner solar system. Annual Reviews of Earth
1103 and Planetary Sciences, 40, 113-139.

1104 Elkins-Tanton, L.T., Burgess, S., and Yin, Q.Z. (2011) The lunar magma ocean: Reconciling the
1105 solidification process with lunar petrology and geochronology. Earth and Planetary Science
1106 Letters, 304, 326-336.
1107 Ereshefsky, M. (2014) Species, historicity, and path dependency. Philosophy of Science, 81,
1108 714-726.
1109 Ernst, W.G., Sleep, N.H., and Tsujimori, T. (2016) Plate-tectonic evolution of the Earth: Bottom-
1110 up and top-down mantle circulation. Canadian Journal of Earth Science, 53, 1103-1120.
1111 Essene, E.J., and Fisher, D.C. (1986) Lightning strike fusion: Extreme reduction and metal-
1112 silicate immiscibility. Science, 234, 189-193.
1113 Evans, A.J., Andrews-Hanna, J.C., Head, J.W. III, Soderblom, J.M., Solomon, S.C., and Zuber,
1114 M.T. (2018) Reexamination of early lunar chronology with GRAIL data: Terranes, basins,
1115 and impact fluxes. Journal of Geophysical Research: Planets, 123, (22 p.),
1116 https://doi.org/10.1029/2017JE005421.
1117 Faure, F., Arndt, N., and Libourel, G. (2006) Formation of spinifex texture in komatiites: an
1118 experimental study. Journal of Petrology, 47, 1591-1610.
1119 Feng, T., Gull, M., Omran, A., Abbott-Lyon, H., and Pasek, M.A. (2021) The evolution of
1120 ephemeral phosphate minerals on planetary environments. ACS Earth and Space Chemistry,
1121 5, 1647-1656.
1122 Fenner, C.N. (1929) The crystallization of basalts. American Journal of Science, 18, 225-253.
1123 Fleet, M.E. (2003) Rock-Forming Minerals. Volume 3A, Second Edition. Sheet Silicates: Micas.
1124 The Geological Society of London.
1125 Furnes, H., and Dilek, Y. (2017) Geochemical characterization and petrogenesis of intermediate
1126 to silicic rocks in ophiolites: A global synthesis. Earth-Science Reviews, 166, 1-37.

1127 Gaillard, F., and Scaillet, B. (2014) A theoretical framework for volcanic degassing chemistry in
1128 a comparartive planetology perspective and implications for planetary atmospheres. Earth and
1129 Planetary Science Letters, 403, 307-316.
1130 Giampouras, M., Garrido, C.J., Bach, W., Los, C., Fussmann, D., Monien, P., and Garcia-Ruiz,
1131 J.M. (2020) On the controls of mineral assemblages and textures in alkaline sporings, Samail
1132 Ophiolite, Oman. Chemical Geology, 533, 119435 (22 p.).
1133 Glass, B.P., Liu, S., and Leavens, P.B. (2002) Reidite: an impact-produced high-pressure
1134 polymorph of zircon found in marine sediments. American Mineralogist, 87, 562-565.
1135 Godman, M. (2019) Scientific realism with historical essences: The case of species. Synthese,
1136 https://doi.org/10.1007/s11229-018-02034-3.
1137 Grapes, R. (2006) Pyrometamorphism. Second Edition. Springer.
1138 Green, D.H. (1975) Genesis of Archean peridotitic magmas and constraints on Archean
1139 geothermal gradients and tectonics. Geology, 3, 15-18.
1140 Gregory, D.D., Cracknell, M.J., Large, R.R., McGoldrick, P., Kuhn, S., Maslennikov, V.V.,
1141 Baker, M.J., Fox, N., Belousov, I., Figueroa, M.C., Steadman, J.A., Fabris, A.J., and Lyons,
1142 T.W. (2019) Distinguishing ore deposit type and barren sedimentary pyrite using laser
1143 ablation-inductively coupled plasma-mass spectrometry trace element data and statistical
1144 analysis of large data sets. Economic Geology, 114, 771-786.
1145 Grieve, R.A.F., Cintala, M.J., and Therriault, A.M. (2006) Large-scale impacts and the evolution
1146 of the Earth's crust: The early years. In: W.U. Reimold and R.L. Gibson, Eds., Processes of
1147 the Early Earth, Geological Society of America Special Paper, 405, 23-31.

1148 Griffin, W.L., Belousova, E.A., O'Neill, C., O'Reilly, S.Y., Malkovets, V., Pearson, N.J.,
1149 Spetsius, S., and Wilde, S.A. (2014) The World Turns Over: Hadean – Archean crust-mantle
1150 evolution. Lithos, 189, 2-15.
1151 Griffin, W.L., Afonso, J.C., Belousova, E.A., Gain, S.E., Gong, X.-H., Gonzáles-Jiménez, J.M.,
1152 Howell, D., Huang, J.-X., McGowan, N., Pearson, N.J., and others (2016) Mantle recycling:
1153 Transition zone metamorphism of Tibetan ophiolitic peridotites and its tectonic implications.
1154 Journal of Petrology, 57, 655-684.
1155 Griffin, W.L., Howell, D., Gonzáles-Jiménez, J.M., Xiong, Q., and O'Reilly, S.Y. (2018)
1156 Comment on "Ultra-high pressure and ultra-reduced minerals in ophiolites may form by
1157 lightning strikes" by Ballhaus et al. (2017): Ultra-high pressure and super-reduced minerals in
1158 ophiolites do not form by lightning strikes. Geochemical Perspective Letters, 7, 1-2
1159 Guilbert, J.M., and Park, C.F., Jr. (2007) The Geology of Ore Deposits. Waveland Press.
1160 Hamilton, W.B. (2007) Earth's first two billion years—The era of internally mobile crust.
1161 Geological Society of America Memoir, 200, 233-296.
1162 Harrison, T.M. (2009) The Hadean crust: Evidence from > 4 Ga zircons. Annual Review of
1163 Earth and Planetary Sciences, 37, 479-505.
1164 Harrison, T.M., Blichert-Toft, J., Müller, W., Albarede, F., Holden, P., and Mojzsis, S.J. (2005)
1165 Heterogeneous Hadean hafnium: Evidence of continental crust at 4.4 to 4.5 Ga. Science, 310,
1166 1947–1950.
1167 Harrison, T.M., Schmitt, A.K., McCulloch, M.T., and Lovera, O.M. (2008) Early (> 4.5 Ga)
1168 formation of terrestrial crust: Lu-Hf, $\delta^{18}O$, and Ti thermometry results for Hadean zircons.
1169 Earth and Planetary Science Letters, 268, 476–486.

Hatert, F., Mills, S.J., Hawthorne, F.C., and Rumsey, M.S. (2021) A comment on "An evolutionary system of mineralogy: Proposal for a classification of planetary materials based on natural kind clustering." American Mineralogist, 106, 150-153.

Hawley, K., and Bird, A. (2011) What are natural kinds? Philosophical Perspectives, 25, 205-221.

Hawthorne, F.C., Mills, S.J., Hatert, F., and Rumsey, M.S. (2021) Ontology, archetypes and the definition of "mineral species." Mineralogical Magazine, 85, 125-131.

Haymon, R.M., and Kastner, M. (1981) Hot spring deposits on the East Pacific Rise at 21°N: Preliminary description of mineralogy and genesis. Earth and Planetary Science Letters, 53, 363-381.

Hazen, R.M. (2013) Paleomineralogy of the Hadean Eon: A preliminary list. American Journal of Science, 313, 807-843.

Hazen, R.M. (2019) An evolutionary system of mineralogy: Proposal for a classification based on natural kind clustering. American Mineralogist, 104, 810-816.

Hazen, R.M. (2021) Reply to "A comment on 'An evolutionary system of mineralogy: Proposal for a classification of planetary materials based on natural kind clustering'." American Mineralogist, 106, 154-156.

Hazen, R.M., and Ausubel, J.H. (2016) On the nature and significance of rarity in mineralogy. American Mineralogist, 101, 1245-1251.

Hazen, R.M., and Morrison, S.M. (2020) An evolutionary system of mineralogy, Part I: stellar mineralogy (>13 to 4.6 Ga). American Mineralogist, 105, 627-651.

Hazen, R.M., and Morrison, S.M. (2021a) An evolutionary system of mineralogy, Part V: Planetesimal Aqueous and thermal alteration of planetesimals (4.565 to 4.550 Ga). American Mineralogist, 106, in press. https://doi.org/10.2138/am-2021-7760

Hazen, R.M., and Morrison, S.M. (2021b) Mineralogical environments of the Hadean Eon: Templates for the Origins of Life? In: A. Neubeck and S. McMahon, Eds., Prebiotic Chemistry and the Origin of Life. Springer. In press.

Hazen, R.M., and Morrison, S.M. (2022) On the paragenetic modes of minerals: A mineral evolution perspective. American Mineralogist, 107, in press.

Hazen, R.M., Morrison, S.M., and Prabhu, A. (2021) An evolutionary system of mineralogy, Part III: Primary chondrule mineralogy (4.566 to 4.561 Ga). American Mineralogist, 106, 325-350.

Hazen, R.M., Morrison, S.M., Krivovichev, S.L., and Downs, R.T. (2022) Lumping and splitting: Toward a classification of mineral natural kinds. American Mineralogist, 107, in press.

Heinrich, C.A., and Henley, R.W. (1989) Hydrothermal Systems. Australian Mineral Foundation.

Hekinian, R., Fevrier, M., Bischoff, J.L., Picot, P., and Shanks, W.C. (1980) Sulfide deposits from the East Pacific Rise near 21 N. Science, 207, 1433-1444.

Hess, B.L., Piazolo, S., and Harvey, J. (2021) Lightning strikes as a major facilitator of prebiotic phosphorus reduction on early Earth. Nature Communications, 12, Article #1535.

Hickman, A.H., and Van Kranendonk, M.J. (2012) Early Earth evolution: Evidence from the 3.5-1.8 Ga geological history of the Pilbara region of Western Australia. Episodes, 35, 283-297.

Holland, H.D. (1984) The Chemical Evolution of the Atmosphere and Oceans. Princeton University Press.

1214 Holm, N.G., Oze, C., Mousis, O., Waite, J.H., and Guilbert-Lepoutre, A. (2015) Serpentinization
1215 and the formation of H_2 and CH_4 on celestial bodies (planets, moons, comets). Astrobiology,
1216 2015, 587-600.
1217 Holser, W.T. (1979) Mineralogy of evaporites. Reviews in Mineralogy, 6, 213-294.
1218 Hui, H., Peslier, A.H., Zhang, Y., and Neal, C.R. (2013) Water in lunar anorthosites and
1219 evidence for a wet early Moon. Nature Geoscience, 6, 177-180.
1220 Ikoma, M., Elkins-Tanton, L., Hamano, K., and Suckale, J. (2018) Water partitioning in
1221 planetary embryos and protoplanets with magma oceans. Space Science Reviews, 214, 76 (28
1222 p.)
1223 Isley, A.E., and Abbott, D.H. (1999) Plume-related mafic volcanism and the deposition of
1224 banded iron formation. Journal of Geophysical Research, 104, 5,461–15,477.
1225 Izawa, M.R.M., Nesbitt, H.W., MacRae, N.D., and Hoffman, E.L. (2010) Composition and
1226 evolution of the early oceans: Evidence from the Tagish Lake meteorite. Earth and Planetary
1227 Science Letters, 298, 443-449.
1228 Jarrard, R.D. (2003) Subduction fluxes of water, carbon dioxide, chlorine, and potassium.
1229 Geochemistry Geophysics Geosystems, 4, 8905.
1230 Johannsen, A. (1932) A Descriptive Petrography of the Igneous Rocks. Volume II. The Quartz-
1231 Bearing Rocks. The University of Chicago Press.
1232 Johannsen, A. (1937) A Descriptive Petrography of the Igneous Rocks. Volume III. The
1233 Intermediate Rocks. The University of Chicago Press.
1234 Johannsen, A. (1938) A Descriptive Petrography of the Igneous Rocks. Volume IV. Part I: The
1235 Feldspathoid Rocks. Part II: The Peridotites and Perknites. The University of Chicago Press.

1236 Jolliff, B.L., Wieczorek, M.A., Shearer, C.K., and Neal, C.R. (2006) New Views of the Moon.
1237 Reviews in Mineralogy and Geochemistry, 60. Mineralogical Society of America.
1238 Jolliff, B.L., Wiseman, S.A., Lawrence, S.J., Tran, T.N., Robinson, M.S., Sato, H., Hawke, B.R.,
1239 Scholten, F., Oberst, J., Hiesinger, H., van der Bogert, C.H., Greenhagen, B.T., Glotch, T.D.,
1240 and Paige, D.A. (2011) Non-mare silicic volcanism on the lunar farside at Compton-
1241 Belkovich. Nature Geoscience, 4, 566–571.
1242 Kadoya, S., Krissansen-Totton, J., and Catling, D.C. (2020) Probable cold and alkaline surface
1243 environment of the Hadean Earth caused by impact ejecta weathering. Geochemistry
1244 Geophysics Geosystems, 21, e2019GC008734 (18 p.).
1245 Kasting, J.F., and Howard, M.T. (2006) Atmospheric composition and climate on the early
1246 Earth. Philosophical Transactions of the Royal Society of London B Biological Sciences, 361,
1247 1733-1742.
1248 Kawai, K., Tsuchiya, T., Tsuchiya, J., and Maruyama, S. (2009) Lost primordial continents.
1249 Gondwana Research, 16, 581-586.
1250 Kelemen, P.B., and Matter, J. (2008) In situ carbonation of peridotite for CO_2 storage.
1251 Proceedings of the National Academy of Sciences, 105, 17295-17300.
1252 Kemp, A.I.S., Wilde, S.A., Hawkesworth, C.J., Coath, C.D., Nemchin, A., Pidgeon, R.T.,
1253 Vervoort, J.D., and DuFrame, S.A. (2010) Hadean crustal evolution revisited: New
1254 constraints from Pb–Hf isotope systematics of the Jack Hills zircons. Earth and Planetary
1255 Science Letters, 296, 45–56.
1256 Khalidi, M.A. (2013) Natural Categories and Human Kinds: Classification in the Natural and
1257 Social Sciences. Cambridge University Press.

1258 Kim, J.D., Yee, N., Nanda, V., and Falkowski, P.G. (2013) Anoxic photochemical oxidation of
1259 siderite generates molecular hydrogen and iron oxides. Proceedings of the National Academy
1260 of Sciences USA, 110, 10073-10077.
1261 Kim, H., Furukawa, Y., Kakegawa, T., Bita, A., Scorei, R., and Benner, S.A. (2016) Evaporite
1262 borate-containing mineral ensembles make phosphate available and regiospecifically
1263 phosphorylate ribonucleosides: Borate as a multifaceted problem solver in prebiotic
1264 chemistry. Angewalte Chemie International Edition, 55, 15816–15820.
1265 Kinzler, R.J., and Grove, T.L. (1992) Primary magmas of midocean ridge basalts 1. Experiments
1266 and methods. Journal of Geophysical Research, 97, 6885–6906.
1267 Kohn, S.C., and Grant, K.J. (2006) The partitioning of water between nominally anhydrous
1268 minerals and silicate melts. Reviews in Mineralogy and Geochemistry, 62, 231–241.
1269 Knauth, L.P. (2005) Temperature and salinity history of the Precambrian ocean: Implications for
1270 the course of microbial evolution. Paleogeography Paleoclimatology Paleoecology, 219, 53-
1271 69.
1272 Koeberl, C. (2002) Mineralogical and geochemical aspects of impact craters. Mineralogical
1273 Magazine, 66, 745-768.
1274 Koeberl, C. (2006) Impact processes on the early Earth. Elements, 2, 211-216.
1275 Korenaga, J. (2008) Plate tectonics, flood basalts, and the evolution of Earth's oceans. Terra
1276 Nova, 20, 419–439.
1277 Korenaga, J. (2021) Hadean geodynamics and the nature of early continental crust. Precambrian
1278 Research, 359, 106178 (28 p.).

Korenaga, J., Planavsky, N.J., and Evans, D.A.D. (2017) Global water cycle and the coevolution of Earth's interior and surface environment. Philosophical Transactions of the Royal Society, A375, 20150393.

Kruijer, T.S., Touboul, M., Fischer-Godde, M., Bermingham, K.R., and Kleine, T. (2014) Protracted core formation and rapid accretion of protoplanets. Science, 344, 1150-1154.

Kruijer, T.S., Burkhardt, C., Budde, G., and Kleine, T. (2017) Age of Jupiter from the distinct genetics and formation times of meteorites. Proceedings of the National Academy of Sciences USA. Doi: 10.1073/pnas.1704461114

Kuritani, T., Yoshida, T., Kimura, J.-I., Hirahara, Y., and Takahashi, T. (2014) Water content of primitive low-K tholeiitic basalt magma from Iwate Volcano, NE Japan arc: Implications for differentiation mechanism of frontal-arc basalt magmas. Mineralogy and Petrology, 108, 1-11.

Kurokawa, H., Foriel, J., Laneuville, M., Houser, C., and Usui, T. (2018) Subduction and atmospheric escape of Earth's seawater constrained by hydrogen isotopes. Earth and Planetary Science Letters, 497, 149–160.

Lamadrid, H.M., Rimstidt, J.D., Schwarzenbach, E.M., Klein, F., Ulrich, S., Dolocan, A., and Bodnar, R.J. (2017) Effect of water activity on rates of serpentinization of olivine. Nature Communications, 8, 16107 (9 p.).

Lambart, S.L., Baker, M.B., and Stolper, E.M. (2016) The role of pyroxenite in basalt genesis: Melt-PX, a melting parameterization for mantle pyroxenites between 0.9 and 5 GPa. Journal of Geophysical Research – Solid Earth, 121, 5708-5735.

Lebrun, T., Massol, H., Chassefiere, E., Davaille, A., Marcq, E., Sarda, P., Leblanc, F., and Brandeis, G. (2013) Thermal evolution of an early magma ocean in interaction with the atmosphere. Journal of Geophysical Research Planets, 118, 1155–1176.

Lin, Y., Trnoche, E.J., Steenstra, E.S., and van Westrenen, W. (2017) Experimental contsraints on the solidification of a nominally dry lunar magma ocean. Earth and Planetary Science Letters, 471, 104-116.

Lock, S.J., Stewart, S.T., Petaev, M.L., Leinhardt, Z., Mace, M.T., Jacobsen, S.B., and Ćuk, M. (2018) The origin of the Moon within a terrestrial synestia. Journal of Geophysical Research: Planets, 123, 910-953.

Lock, S.J., Stewart, S.T., and Ćuk, M. (2020) The energy budget and figure of Earth during recovery from the Moon-forming impact. Earth and Planetary Science Letters, 530, 115885 (11 p.)

London, D. (2008) Pegmatites. Mineralogical Assocxiation of Canada.

Longhi, J., Durand, S.R., and Walker, D. (2010) The pattern of Ni and Co abundances in lunar olivines. Geochemica et Cosmochimica Acta, 74, 784-798.

Lorenz, R.D. (2018) Lightning detection on Venus: A critical review. Progress in Earth and Planetary Science, 5, 34 (25 p.).

Lowell, R.P., and Rona, P.A. (2002) Seafloor hydrothermal systems driven by the serpentinization of peridotite. Geophysical Research Letters, 29, 1-5.

Ma, C. (2018) A closer look at shock meteorites: Discovery of new high-pressure minerals. American Mineralogist, 103, 1521-1522.

Ma, C., Tschauner, O., and Beckett, J.R. (2019a) Discovery of a new high-pressure silicate phase, $(Fe,Mg,Cr,Ti,Ca,\square)_2(Si,Al)O_4$ with a tetragonal spinelloid structure, in a shock melt

pocket from the Tissint Martian meteorite. Lunar and Planetary Science Conference, 50, 1460.

Ma, C., Tschauner, O., Bindi, L., Beckett, J.R., and Xie, X. (2019b) A vacancy-rich, partially inverted spinelloid silicate, $(Mg,Fe,Si)_2(Si,\square)O_4$, as a major matrix phase in shock melt veins of the Tenham and Suizhou L6 chondrites. Meteoritics & Planetary Science, 54, 1907-1918.

Magnus, P.D. (2012) Scientific Enquiry and Natural Kinds: From Mallards to Planets. Palgrave MacMillan.

Maier, W.D. (2005) Platinum-group element (PGE) deposits and occurrences: Mineralization styles, genetic concepts, and exploration criteria. Journal of African Earth Science, 41, 165–191.

Marchi, S., Bottke, W.F., Elkins-Tanton, L.T., Wuennemann, K., Morbidelli, A., Kring, D.A. (2014) Widespread mixing and burial of Earth's Hadean crust by asteroid impacts. Nature, 511, 578-582.

Marks, M.A.W., and Markl, G. (2017) A global review on agpaitic rocks. Earth Science Reviews, 173, 229-258.

Martin, H., and Moyen, J.-F. (2002) Secular changes in TTG composition as markers of the progressive cooling of the Earth. Geology, 30, 319–322.

Martin, H., Smithies, R.H., Rapp, R., Moyen, J.-F., and Champion, D. (2005) An overview of adakite, tonalite-trondhjemite-granodiorite (TTG), and sanukitoid—Relationships and some implications for crustal evolution. Lithos, 79, 1–24,

Marty, B., Avice, G., Bekaert, D.V., and Broadley, M.W. (2018) Salinity of the Archean oceans from analysis of fluid inclusions in quartz. Comptes Rendus Geoscience, 350, 154-163.

1345 Maruyama, S., and Ebisuzaki, T. (2017) Origin of the Earth: A proposal of new model called
1346 ABEL. Geoscience Frontiers, 8, 253-274.
1347 Maruyama, S., Ikoma, M., Genda, H., Hirose, K., Yokoyama, T., and Santosh, M. (2013) The
1348 naked planet Earth: Most essential pre-requisite for the origin and evolution of life.
1349 Geoscience Frontiers, 4, 141-165.
1350 Matsui, T., and Abe, Y. (1986) Formation of a "magma ocean" on the terrestrial planets due to
1351 the blanketing effect of an impact-induced atmosphere. Earth Moon Planets, 34, 223–230.
1352 McNutt, S.R., and Williams, E.R. (2010) Volcanic lightning: Global observations and constraints
1353 on source mechanisms. Bulletin of Volcanology, 72, 1153–1167.
1354 Mills, S.J., Hatert, F., Nickel, E.H., and Ferrais, G. (2009) The standardization of mineral group
1355 hierarchies: Application to recent nomenclature proposals. European Journal of Mineralogy,
1356 21, 1073-1080.
1357 Miyazaki, Y., and Korenaga, J. (2019a) On the timescale of magma ocean solidification and its
1358 chemical consequences: 1. Thermodynamic database for liquid at high pressures. Journal of
1359 Geophysical Research Solid Earth, 124, 3382-3398.
1360 Miyazaki, Y., and Korenaga, J. (2019b) On the timescale of magma ocean solidification and its
1361 chemical consequences: 2. Compositional differentiation under crustal accumulation and
1362 matrix compaction. Journal of Geophysical Research Solid Earth, 124, 3399-3419.
1363 Mojzsis, S.J., Harrison, T.M., and Pidgeon, R.T. (2001) Oxygen-isotope evidence 1831 from
1364 ancient zircons for liquid water at the Earth's surface 4,300 Myr ago. Nature, 409, 178–181.
1365 Moody, J. (1976) Serpentinization: A review. Lithos, 9, 125-138.
1366 Moore, J.G. (1970) Water content of basalt erupted on the ocean floor. Contributions to
1367 Mineralogy and Petrology, 28, 272-279.

1368 Morbidelli, A., Nesvorny, D., Laurenz, V. Marchi, S., Rubie, D.C., Elkins-Tanton, L.,
1369 Wieczorek, M., and Jacobson, S. (2018) The timeline of the lunar bombardment: Revisted.
1370 Icarus, 305, 262-276.
1371 Morrison, S.M., and Hazen, R.M. (2020) An evolutionary system of mineralogy, part II:
1372 interstellar and solar nebula primary condensation mineralogy (> 4.565 Ga). American
1373 Mineralogist, 195, 1508-1535.
1374 Morrison, S.M., and Hazen, R.M. (2021) An evolutionary system of mineralogy, part IV:
1375 Planetesimal differentiation and impact mineralization (4.566 to 4.560 Ga). American
1376 Mineralogist, 106, 730-761.
1377 Morrison, S.M., Liu, C., Eleish, A., Prabhu, A., Li, C., Ralph, J., Downs, R.T., Golden, J.J., Fox,
1378 P., Hummer, D.R., Meyer, M.B., and Hazen, R.M. (2017) Network analysis of mineralogical
1379 systems. American Mineralogist, 102, 1588-1596.
1380 Morrison, S.M., Runyon, S.E., and Hazen, R.M. (2018) The paleomineralogy of the Hadean Eon
1381 revisited. Life, 8, 64 (20 p.).
1382 Morse, S.A. (1986) Origin of earliest planetary crust: role of compositional convection. Earth
1383 and Planetary Science Letters, 81, 118–126.
1384 Morse, J.W., and Mackenzie, F.T. (1998) Hadean ocean carbonate chemistry. Aquatic
1385 Geochemistry, 4, 301-319.
1386 Moynier, F., Yin, Q.-Z., Boyet, M., Jacobsen, B., and Rosing, M.T. (2010) Coupled ^{182}W-^{142}Nd
1387 constraint for early Earth differentiation. Proceedings of the National Academy of Sciences
1388 USA, 107, 10810-10814.
1389 Mungall, J.E., and Naldrett, A.J. (2008) Ore deposits of the platinum-group elements. Elements,
1390 4, 253-258.

Norman, M.D., Borg, L.E., Nyquist, L.E., and Bogard, D.D. (2003) Chronology, geochemistry, and petrology of a ferroan noritic anorthosite clast from Descartes breccia 67215: Clues to the age, origin, structure, and impact history of the lunar crust. Meteoritics & Planetary Science, 38, 645-661.

Ohtani, E., Kimura, Y., Kimura, M., Takata, T., Kondo, T., and Kubo, T. (2004) Formation of high-pressure minerals in shocked L6 chondrite Yamato 791384: Constraints on shock conditions and parent body size. Earth and Planetary Science Letters, 227, 505–515.

O'Neil, J., and Carlson, R.W. (2017) Building Archean cratons from Hadean mafic crust. Science, 355, 1199–1202.

O'Neill, C., and Debaille, V. (2014) The evolution of Hadean-Eoarchean geodynamics. Earth and Planetary Science Letters, 406, 49-58.

O'Neil, J., Carlson, R.W., Francis, D., and Stevenson, R.K. (2008) Neodymium-142 evidence for Hadean mafic crust. Science, 321, 1828–1831.

O'Neil, J., Francis, D., and Carlson, R.W. (2011) Implications of the Nuvvuagittuq greenstone belt for the formation of Earth's early crust. Journal of Petrology, 52, 985-1009.

Osinski, G.R., Tornabene, L.L., Banerjee, N.R., Cockell, C.S., Flemming, R., Izawa, M.R.M., McCutcheon, J., Parnell, J., Preston, L.J., Pickersgill, A.E., Pontefract, A., Sapers, H.M., and Southam, G. (2013) Impact-generated hydrothermal systems on Earth and Mars. Icarus, 224, 347–363.

Palandri, J.L., and Reed, M.H. (2004) Geochemical models of metasomatism in ultramafic systems: Serpentinization, rodingitization, and sea floor carbonate chimney precipitation. Geochimica et Cosmochimica Acta, 68, 1115- 1133.

1413 Pasek, M.A., and Block, K. (2009) Lightning-induced reduction of phosphorus oxidation state.
1414 Nature Geoscience, 2, 553-556.
1415 Pasek, M.A., Block, K., and Pasek, V. (2012) Fulgurite morphology: A classification scheme and
1416 clues to formation. Contributions to Mineralogy and Petrology, 164, 477-492.
1417 Philpotts, A.R., and Ague, J.J. (2009) Principles of Igneous and Metamorphic Petrology. Second
1418 Edition. Cambridge University Press.
1419 Pietranik, A.B., Hawkesworth, C.J., Storey, C.D., Kemp, A.I.S., Sircombe, K.N., Whitehouse,
1420 M.J., and Bleeker, W. (2008) Episodic mafic crust formation from 4.5–2.8 Ga: New evidence
1421 from detrital zircons, Slave Craton, Canada. Geology, 36, 875–878.
1422 Pilchin, A., and Eppelbaum, L. (2012) The early Earth, formation and evolution of the
1423 lithosphere in the Hadean—Middle Archean. Encyclopedia of Earth Science Research, 1, 1-
1424 94.
1425 Pirajno, F. (2009) Hydrothermal Processes and Mineral Systems. Springer.
1426 Pirajno, F. (2020) Subaerial hot springs and near-surface hydrothermal mineral systems past and
1427 present, and possible extraterrestrial analogues. Geoscience Frontiers, 11, 1549-1569.
1428 Ricardo, A., Carrigan, M.A., Olcott, A.N., and Benner, S.A. (2004) Borate minerals stabilize
1429 ribose. Science, 303, 196.
1430 Righter, K., and Drake, M.J. (1999) Effect of water on metal-silicate partitioning of siderophile
1431 elements a high pressure and temperature terrestrial magma ocean and core formation. Earth
1432 and Planetary Science Letters, 171, 383–399.
1433 Roberts, A.C., Ansell, H.G., and Bonardi, M. (1980) Pararealgar, a new polymorph of AsS, from
1434 British Columbia. Canadian Mineralogist, 18, 525–527.

Rodriguez, J.A.P., Sasaki, S., Dohm, J.M., Tanaka, K.L., Strom, B., Kargel, J., Kuzmin, R., Miyamoto, H., Spray, J.G., Fairén, A.G., Komatsu, G., Kurita, K., and Baker, V. (2005) Control of impact crater fracture systems on subsurface hydrology, ground subsidence, and collapse, Mars. Journal of Geophysical Research, 110, E06003 (22 p.).

Rollinson, H. (2007) Early Earth Systems: A Geochemical Approach. Blackwell Publishing.

Rosas, J.C., and Korenaga, J. (2021) Archean seafloor shallowed with age due to radiogenic heating in the mantle. Nature Geoscience, 14, 51–56.

Rubin, A.E., and Ma, C. (2021) Meteorite Mineralogy. Cambridge University Press.

Russell, M.J., Hall, A.J., and Martin, W. (2010) Serpentinization as a source of energy at the origin of life. Geobiology, 8, 355-371.

Russell, C.T., Strangeway, R.J., Daniels, J.T.M., Zhang, T.L., and Wei, H.Y. (2011) Venus lightning: Comparison with terrestrial lightning. Planetary and Space Science, 59, 965-973.

Russell, C.T., Zhang, T.L., and Wei, H.Y. (2008) Whistler mode waves from lightning on Venus: Magnetic control of ionospheric access. Journal of Geophysical Research, 113, E00B05.

Saal, A.E., Hauri, E.H., Cascio, M.L., Van Orman, J.A., Rutherford, M.C., and Cooper, R.F. (2008) Volatile content of lunar volcanic glasses and the presence of water in the Moon's interior. Nature, 454, 192-195.

Schaefer, L., and Elkins-Tanton, L.T. (2018) Magma oceans as a critical stage in the tectonic development of rocky planets. Philosophical Transactions of the Royal Society London A, 376, 20180109, (17 p.)

Schaefer, L., and Fegley, B. Jr. (2010) Chemistry of atmospheres formed during accretion of the Earth and terrestrial planets. Icarus, 208, 438-448.

1458 Schertl, H.-P., Mills, S.J., and Maresch, W.V. (2018) A Compendium of IMA-Approved Mineral
1459 Nomenclature. International Mineralogical Association.
1460 Schwarzenbach, E.M., and Steele-MacInnis, M. (2020) Fluids in submarine mid-ocean ridge
1461 hydrothermal settings. Elements, 16, 389-394.
1462 Sekine, Y., Sugita, S., Kadono, T., and Matsui, T. (2003) Methane production by large iron
1463 meteorite impacts on early Earth. Journal of Geophysical Research, 108, 5070-5075.
1464 Sharkov, E.V., and Bogina, M.M. (2009) Mafic-ultramafic magmatism of the Early Precambrian
1465 (from Archean to Paleoproterozoic). Stratigraphy and Geological Correlations, 17, 17-136.
1466 Shibuya, T., Yoshizaki, M., Masaki, Y., Suzuki, K., Takai, K., and Russell, M.J. (2013)
1467 Reactions between basalt and CO_2-rich seawater at 250 and 350 ºC, 500 bars: Implications for
1468 the CO_2 sequestration into the modern oceanic crust and the composition of hydrothermal
1469 vent fluid on the CO_2-rich early ocean. Chemical Geology, 359, 1-9.
1470 Shibuya, T., Yoshizaki, M., Sat, M., Shimizu, K., Nakamura, K., Omon, S., Suzuki, K., Takai,
1471 K., Tsunakawa, H., and Maruyama, S. (2015) Hydrogen-rich hydrothermal environments in
1472 the Hadean ocean inferred from serpentinization of komatiites at 300 ºC and 500 bar. Progress
1473 in Earth and Planetary Science, 2, 46 (11 p.).
1474 Shore, M., and Fowler, A.D. (1999) The origin of spinifex texture in komatiites. Nature, 397,
1475 691-694.
1476 Shrenk, M.O., Brazelton, W.J., and Lang, S.Q. (2013) Serpentinization, carbon, and deep life.
1477 Reviews in Mineralogy and Geochemistry, 75, 575-606.
1478 Sleep, N.H., and Zahnle, K. (2001) Carbon dioxide cycling and implications for climate on
1479 ancient Earth. Journal of Geophysical Research, 106, 1373-1399.

Smith, C.M., Gaudin, D., Van Eaton, A.R., Behnke, S.A., Reader, S., Thomas, R.J., Edens, H., McNutt, S.R., and Cimarelli, C. (2021) Impulsive volcanic plumes generate volcanic lightning and vent discharges: A statistical analysis of Sakurajima volcano in 2015. Geophysical Research Letters, 48, e2020GL092323, (10 p.).

Snyder, G.A., Taylor, L.A., and Neal, C.R. (1992) A chemical model for generating the sources of mare basalts: Combined equilibrium and fractional crystallization of the lunar magmasphere. Geochemical et Cosmochimica Acta, 56, 3809-3821.

Solomatov, V.S. (2000) Fluid dynamics of a terrestrial magma ocean. In R.M. Canup and K. Righter, Eds., Origin of the Earth and Moon, pp. 323–338. University of Arizona Press.

Solomatov, V.S. (2007) Magma oceans and primordial mantle differentiation. Treatise on Geophysics, 9, 91–119.

Solomatov, V.S., and Stevenson, D.J. (1993a) Kinetics of crystal growth in a terrestrial magma ocean. Journal of Geophysical Research, 98, 5407–5418.

Solomatov, V.S., and Stevenson, D.J. (1993b) Nonfractional crystallization of a terrestrial magma ocean. Journal of Geophysical Research, 98, 5391–5406.

Solomatov, V.S., and Stevenson, D.J. (1993c) Suspension in convective layers and style of differentiation of a terrestrial magma ocean. Journal of Geophysical Research, 98, 5375–5390.

Solomatov, V.S., Olson, P., and Stevenson, D.J. (1993) Entrainment from a bed of particles by thermal convection. Earth and Planetary Science Letters, 120, 387–393.

Solomon, S. (1979) Formation, history, and energetics of cores in the terrestrial planets. Physics of Earth and Planetary Interiors, 19, 168–182.

Stevenson, D.J. (1987) Origin of the Moon—The collision hypothesis. Annual Review of Earth and Planetary Sciences, 15, 271–315.

1503 Stöffler, D., Hamann C., and Metzler K. (2018) Shock metamorphism of planetary silicate rocks
1504 and sediments: Proposal for an updated classification system. Meteoritics & Planetary
1505 Science, 53, 5-49.
1506 Streit, E., Kelemen, P., and Eiler, J. (2012) Coexisting serpentine and quartz from carbonate-
1507 bearing serpentinized peridotite in the Samail Ophiolite, Oman. Contributions to Mineralogy
1508 and Petrology, 164, 821-837.
1509 Taylor, S.R. (1982) Planetary Science: A Lunar Perspective. Lunar and Planetary Institute.
1510 Taylor, S.R., and McLennan, S.M. (1985) The Continental Crust: Its Composition and Evolution.
1511 Blackwell.
1512 Thiemens, M.M., Sprung, P., Fonseca, R.O.C., Leitzke, F.P., and Munker, C. (2019) Early Moon
1513 formation inferred from hafnium-tungsten systematics. Nature Geosciences, 12, 696–700.
1514 Tikoo, S.M., and Elkins-Tanton, L.T. (2017) The fate of water within Earth and super-Earths and
1515 implications for plate tectonics. Philosophical Transactions of the Royal Society of London A,
1516 375, 20150394 (18 p.).
1517 Tomioka, N., and Miyahara, M. (2017) High-pressure minerals in shocked meteorites:
1518 Meteoritics & Planetary Science, 52, 2017-2039.
1519 Tonks, W.B., and Melosh, H.J. (1990) The physics of crystal settling and suspension in a
1520 turbulent magma ocean. LPI Conference on the Origin of Earth, Oxford University Press, pp.
1521 151-174.
1522 Tonks, W.B., and Melosh, H.J. (1993) Magma ocean formation due to giant impacts. Journal of
1523 Geophysical Research, 98, 5319–5333.

1524 Trønnes, R.G., Baron, M.A., Eigenmann, K.R., Guren, M.G., Heyn, B.H., Løken, A., and Mohn,
1525 C.E. (2019) Core formation, mantle differentiation and core-mantle interaction within Earth
1526 and the terrestrial planets. Tectonophysics, 760, 165-198.
1527 Tschauner, O. (2019) High-pressure minerals. American Mineralogist, 104, 1701-1731.
1528 Tschauner, O., Ma, C., Lanzirotti, A., and Newville, M.G. (2020) Riesite, a new high-pressure
1529 polymorph of TiO_2 from the Ries impact structure. Minerals, 10, 78 (8 pp.).
1530 Tucker, J.M., and Mukhopadhyay, S. (2014) Evidence for multiple magma ocean out-gassing
1531 and atmospheric loss episodes from mantle noble gases. Earth and Planetary Science Latters,
1532 393, 254-265.
1533 Valley, J.W., Peck, W.H., King, E.M., Wilde, S.A. (2002) A cool early Earth. Geology, 30, 351-
1534 354.
1535 Valley, J.W., Cavosie, A.J., Ushikubo, T., Reinhard, D.A., Lawrence, D.F., Larson, D.J., Clifton,
1536 P.H., Kelly, T.F., Wilde, S.A., Moser, D.E., and Spicuzza, M.J. (2014) Hadean age for a post-
1537 magma-ocean zircon confirmed by atom-probe tomography. Nature Geoscience, 7, 219-223.
1538 Van Eaton, A.R., Amigo, Á., Bertin, D., Mastin, L.G., Giacosa, R.E., González, J., Valderrama,
1539 O., Fontijn, K., and Behnke, S.A. (2016) Volcanic lightning and plume behavior reveal
1540 evolving hazards during the April 2015 eruption of Calbuco volcano, Chile. Geophysical
1541 Research Letters, 43, 3563–3571.
1542 Van Kranendonk, M.J., Smithies, R.H., and Bennett, V.C. [Editors] (2007) Earth's Oldest Rocks.
1543 Developments in Precambrian Geology, 15. Elsevier.
1544 Vaniman, D.T., and Bish, D.L. (1990) Yoshiokaite, a new Ca,Al-silicate mineral from the Moon.
1545 American Mineralogist, 75, 676-686.

1546 Vergasova, L.P., and Filatov, S.K. (2016) A study of volcanogenic exhalation mineralization.
1547 Journal of Volcanology and Seismology, 10, 71–85.

1548 Voosen, P. (2021) Ancient Earth was a water world. Science, 371, 1088-1089.

1549 Warren, P.H. (1989) Growth of the continental crust: a planetary-mantle perspective.
1550 Tectonophysics, 161, 165–199.

1551 Warren, P.H., Taylor, G.J., Keil, K., Kallemeyn, G.W., Shirley, D.N., and Wasson, J.T. (1983)
1552 Seventh foray: whitlockite-rich lithologies, a diopside-bearing troctolitic anorthosite, ferroan
1553 anorthosites, and KREEP. Proceedings of the 14th Lunar and Planetary Science Conference.
1554 Journal of Geophysical Research, 88, B151–B164.

1555 Wetherill, G.W. (1990) Formation of the Earth. Annual Reviews of Earth and Planetary Science,
1556 18, 205–256.

1557 Wieczorek, M. A., and M. T. Zuber (2001) The composition and origin of the lunar crust:
1558 Constraints from central peaks and crustal thickness modeling, Geophysical Research Letters,
1559 28, 4023–4026.

1560 Wilde, S.A., Valley, J.W., Peck, W.H., and Graham, C.M. (2001) Evidence from detrital zircons
1561 for the existence of continental crust and oceans on Earth 4.4 Gyr ago. Nature, 409, 175-178.

1562 Williams, M.A., and Krider, E.P. (1983) Planetary lightning: Earth, Jupiter, and Venus. Reviews
1563 of Geophysics and Space Physics, 21, 892-902.

1564 Wilson, M.J. (2013) Rock-Forming Minerals. Volume 3C, Second Edition. Sheet Silicates: Clay
1565 Minerals. The Geological Society of London.

1566 Wood et al. (1970) anorthosite crust idea

1567 Xie, Z., Sharp, T.G., and DeCarli, P.S. (2006) High-pressure phases in a shock-induced melt vein
1568 of the Tenham L6 chondrite: Constraints on shock pressure and duration. Geochimica et
1569 Cosmochimica Acta, 70, 504–515.
1570 Yamamoto, S., Nakamura, R., Matsunaga, T., Ogawa, Y., Ishihara, Y., Morotoa, T, Hirata, N.,
1571 Ohtake, M., Hiroi, T., Yokota, Y., and Haruyama, J. (2012) Massive layer of pure anorthosite
1572 on the Moon. Geophysical research Letters, 39, L13201, 6 p.
1573 Yang, J.S., Trumbull, R.B., Robinson, P.T., Xiong, F.H., and Lian, D.Y. (2018) Comment 2 on
1574 "Ultra-high pressure and ultra-reduced minerals in ophiolites may form by lightning strikes."
1575 Geochemical Perspectives Letters, 8, 6-7.
1576 Yoder, H.S. Jr (1976) Generation of Basaltic Magma. National Academy of Sciences Press.
1577 Yoshiya, K., Sato, T., Omori, S., and Maruyama, S. (2018) The birthplace of proto-life: Role of
1578 secondary minerals in forming metallo-proteins through water-rock interaction of Hadean
1579 rocks. Origins of Life and Evolution of Biospheres, 48, 373-393.
1580 Young, E.D., Kohl, I.E., Warren, P.H., Rubie, D.C., Jacobson, S.A., and Morbidelli, A. (2016)
1581 Oxygen isotopic evidence for vigorous mixing during the Moon-forming giant impact.
1582 Science, 351, 493–496.
1583 Zahnle, K.J., Kasting, J.F., and Pollack, J.B. (1988) Evolution of a steam atmosphere during
1584 Earth's accretion. Icarus, 74, 62–97.
1585 Zahnle, K., Arndt, N., Cockell, C., Halliday, A., Nisbet, E., Selsis, F., and Sleep, N.H. (2007)
1586 Emergence of a habitable planet. Space Science Reviews, 29, 35–78.
1587 Zahnle, K.J., Schaefer, L., and Fegley, B. Jr. (2010) Earth's earliest atmospheres. Cold Spring
1588 Harbor Perspectives in Biology, 2010, 2, a004895 (17 p.)

1589 Zahnle, K.J., Lupu, R., Catling, D.C., and Wogin, N. (2020) Creation and evolution of impact-
1590 generated reduced atmospheres of early Earth. The Planetary Science Journal, 1, 11 (21 p.).
1591 Ziegler, E.W., Kim, H.-J., and Benner, S.A. (2018) Molybdenum (VI)-catalyzed rearrangement
1592 of prebiotic carbohydrates in formamide, a candidate prebiotic solvent. Astrobiology, 18,
1593 1159–1170.

1594

This is the peer-reviewed, final accepted version for American Mineralogist, published by the Mineralogical Society of America.
The published version is subject to change. Cite as Authors (Year) Title. American Mineralogist, in press.
DOI: https://doi.org/10.2138/am-2022-8329. http://www.minsocam.org/

Table 1. Distribution of 262 plausible early Hadean (> 4.37 Ga) minerals from 18 near-surface formational environments.

Formational Environment	#Species*	#Cumulative**	Refs***
Primary igneous minerals	*83*		
1. Ultramafic rocks (UMA)	41	41	1,2
2. Mafic rocks (MAF)	39	55	2-4
3. Silica-saturated rocks (SIL)	32	67	4-8
4. Anorthosites (ANO)	15	67	2,3
5. Volcanic fumaroles (FUM)	23	83	9,10
Hydrothermal minerals	*98*		
6. Minerals precipitated in basalt cavities (ZEO)	27	107	11
7. Hydrothermal vein minerals (HYD)	54	139	12
8. Terrestrial hot springs and geysers (HSG)	30	145	11,13,14
9. Seafloor hydrothermal vents (SHT)	32	150	15,16
Thermal or aqueous alteration of prior minerals	*106*		
10. Thermal metamorphism of xenoliths (XEN)	14	152	2,9
11. Serpentinization (SER)	46	178	16-18
12. Low-temperature aqueous alteration (LTA)	67	199	11,13
Surficial mineral-forming processes	*109*		
13. Authigenesis (AUT)	39	201	11,13,19
14. Freezing of aqueous solutions (ICE)	3	204	20
15. Terrestrial impacts (IMP)	41	243	21
16. Lightning (LIG)	12	251	9,22,23
17. Evaporites (EVA)	14	260	24,25
18. Photo-reactions with sunlight (PHO)	5	262	26,27

* Detailed lists of minerals and their paragenetic modes appear in Supplementary Table 1.

** The cumulative total of minerals. Note that many mineral species form by more than one paragenetic process (Hazen and Morrison 2022).

*** General references for mineral formation environments include Anthony et al. (1990-2003); Deer et al. (1982-2013); Hazen and Morrison (2022); and Hazen et al. (2022). See also https://rruff.info/ima and https://mindat.org, and references therein (accessed 7 August 2021).

Numbered references: 1 = Johannsen (1938); 2 = Philpotts and Ague (2009); 3 = Johannsen (1937); 4 = Rollinson (2007); 5 = Johannsen (1932); 6 = Valley et al. (2002); 7 = Hamilton (2007); 8 = Harrison (2008); 9 = Grapes (2006); 10 = Vergasova and Filatov (2016); 11 = Deer et al. (2004); 12 = Mungall and Naldrett (2008); 13 = Wilson (2013); 14 = Pirajno (2020); 15 = Haymond and Kastner (1981); 16 = Palandri and Reed (2004); 17 = Lowell and Rona (2002); 18 = Holm et al. (2015); 19 = Bowles et al. (2011); 20 = Aquioano et al. (2021);

21 = Tschauner (2019); 22 = Essene and Fisher (1986); 23 = Hess et al. (2021); 24 = Holser (1979); 25 = Boggs (2006); 26 = Roberts et al. (1980); 27 = Kim et al. (2013)